A Thesis for the Degree of Master of Science

Comparative approach to decipher the molecular basis of pattern-triggered immunity in *Brassica rapa pekinensis*

배추의 패턴 유발 면역체계의 기반과 기능에 대한 비교 연구

AUGUST 2019

YONGHUA TIAN

MAJOR IN HORTICULTURAL SCIENCE

AND BIOTECHNOLOGY

THE GRADUATE SCHOOL OF

SEOUL NATIONAL UNIVERSITY

Comparative approach to decipher the molecular basis of pattern-triggered immunity in *Brassica rapa pekinensis*

UNDER THE DIRECTION OF DR. CECILE SEGONZAC
SUBMITTED TO THE FACULTY OF THE GRADUATE SCHOOL
SEOUL NATIONAL UNIVERSITY

BY
YONGHUA TIAN

MAJOR IN HORTICULTURAL SCIENCE AND BIOTECHNOLOGY
DEPARTMENT OF PLANT SCIENCE
THE GRADUATE SCHOOL OF SEOUL NATIONAL UNIVERSITY

AUGUST 2019

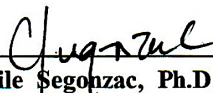APPROVED AS A QUALIFIED THESIS OF YONGHUA TIAN
FOR THE DEGREE OF MASTER OF SCIENCE
BY THE COMMITTEE MEMBERS

CHAIRMAN _____
Doil Choi, Ph.D.

VICE-CHAIRMAN _____
Cecile Segonzac, Ph.D.

MEMBER _____
Byoungcheorl Kang, Ph.D.

Comparative approach to decipher the molecular basis of pattern-triggered immunity in *Brassica rapa pekinensis*

YONGHUA TIAN

DEPARTMENT OF PLANT SCIENCE

THE GRADUATE SCHOOL OF SEOUL NATIONAL UNIVERSITY

ABSTRACT

Chinese cabbage (*Brassica rapa* ssp. *pekinensis*) is an important horticultural crop which is particularly popular in Korea. Several bacterial and fungal diseases can significantly impair Chinese cabbage production. Plants rely on their innate immune system to defend themselves against pathogens. The surface-localized pattern-recognition receptors (PRRs) perceive pathogen-associated molecular patterns (PAMPs), such as flagellin, elongation factor Tu or fungal cell wall component chitin, and induce a series of defense responses called pattern-triggered immunity (PTI). PTI efficiently restricts pathogen growth and provide durable broad-spectrum disease resistance. PRRs and PTI signaling have been intensively investigated in the model species *Arabidopsis thaliana*, however, the comprehensive understanding is scarce in Chinese cabbage.

In order to decipher the molecular basis of PTI in Chinese cabbage, PAMP responsiveness was investigated by assessing typical defense responses. *BraNHL10* was identified as a reliable marker gene whose expression was

significantly and rapidly induced by several PAMPs. ROS production was rapidly induced upon flg22, elf18 and chitin treatments in Chinese cabbage.

Comparative analysis revealed the presence of putative homologs of *Arabidopsis FLS2*, *EFR* and *CERK1* in *B. rapa* genome, and revealed the high similarity between protein sequences of BraPRR and AtPRR. The putative *BraFLS2*, *BraEFR1*, *BraEFR2* and *BraCERK1* were cloned using Golden Gate cloning strategy.

Transient expression of *BraFLS2*, *BraEFRs* and *BraCERK1* in *Nicotiana benthamiana* showed all BraPRRs were plasma membrane-localized and BraFLS2 mediated flg22-triggered endocytosis, BraEFR2 mediated elf18-triggered ROS burst and BraCERK1 led to chitin-independent cell death. *BraEFR1* expression could not induce ROS burst in *N. benthamiana*, suggesting that BraEFR1 might not function.

Subsequently, *BraFLS2*, *BraEFR1*, *BraEFR2* and *BraCERK1* were further characterized by functional complementation in *Arabidopsis fls2* single mutant or *fls2 efr cerk1* triple mutant. The expression of *BraFLS2*, *BraEFR2* and *BraCERK1* conferred gain of flg22, elf18 and chitin-responsiveness, respectively, in transgenic lines. Expression of *BraFLS2* and *BraEFR2* led to flg22 and elf18-induced seedling growth inhibition, respectively, in transgenic *BraFLS2* or *BraEFR2* expressing lines. Expression of *BraFLS2*, *BraEFR2* and *BraCERK1* induced ROS production upon flg22, elf18 and chitin elicitation in transgenic *BraPRR* expressing lines, respectively. Kinase activity of BraPRRs was also assessed in this study via construction of *BraPRR* dead kinase versions.

All results indicated that *BraFLS2*, *BraEFR2* and *BraCERK1* most likely function as PRRs in Chinese cabbage in a partial kinase-dependent manner.

Key words: Chinese cabbage, *Brassica rapa pekinensis*, pattern-triggered immunity (PTI), pattern-recognition receptor (PRR), pathogen-associated molecular pattern (PAMP).

Student number: 2017-20940

CONTENTS

LIST OF TABLES

LIST OF FIGURES

LIST OF ABBREVIATIONS

A. thaliana	*Arabidopsis thaliana*
A. tumefaciens	*Agrobacterium tumefaciens*
AA	Amino Acid residues
At	*Arabidopsis thaliana*
B. rapa	*Brassica rapa pekinensis*
BAK1	BRI1-ASSOCIATED RECEPTOR KINASE 1
BGAL1	β-galactosidase 1
BIK1	BOTRYTIS-INDUCED KINASE 1
BR	brassinosteroids
Bra	*B. rapa*
BRAD	*Brassica* database
CAPS	cleaved amplified polymorphic sequence
CDI1	CELL DEATH INDUCING 1
CDPK	calcium-dependent protein kinase
CEBiP	CHITIN ELICITOR BINDING PROTEIN
CERK1	CHITIN ELICITOR RECEPTOR KINASE 1
Col-0	Columbia

CSP	cold shock protein
dpi	day post infiltration
EFR	EF-TU RECEPTOR
EF-Tu	elongation factor Tu
ER	the endoplasmic reticulum
ETI	effector-triggered immunity
fec	*fls2 efr cerk1* triple mutant
FLS2	FLAGELLIN SENSITIVE 2
FPKM	fragments per kilobase of exon per million fragments mapped
gDNA	genomic DNA
GFP	Green fluorescent protein
HR	hypersensitive response
LD condition	long-day condition
LEC	lectin motifs
LF	less fractioned subgenome
LPS	lipopolysaccharides
LRR domain	leucine-rich repeat domain
LysM	lysine motifs

MAPK	mitogen-activated protein kinase
MF1	moderate fractioned subgenome
MF2	most fractioned subgenome
mod	module
MS medium	Murashige and Skoog medium
N. benthamiana	*Nicotiana benthamiana*
Nb	*Nicotiana benthamiana*
NB domain	nucleotide-binding domain
Norang	Norang Kimchi Baechu
Os	*Oryza sativa*
PAMP	pathogen-associated molecular pattern
PBL	PBS1-LIKE KINASE
PGN	peptidoglycans
PM	plasma membrane
PRR	pattern-recognition receptor
PTI	pattern-triggered immunity
pUC19B	vector pICH41021
qPCR	Quantitative Real-time PCR
qRT-PCR	Quantitative Real-time PCR

R protein	resistance protein
R:S	the ratios of resistant to susceptible individuals
RBOHD	RESPIRATORY BURST OXIDASE HOMOLOG PROTEIN D
Rc	*Rhynchosporium commune*
RLCK	receptor-like cytoplasmic kinase
RLK	receptor-like kinase
RLP	receptor-like protein
RLU	relative light unit
ROS	reactive oxygen species
RT	reverse transcription
RT-PCR	reverse transcription polymerase chain reaction
SD condition	short-day condition
SGI	seedling growth inhibition
SP	signal peptide
TM domain	transmembrane domain
WT	wild-type
YFP	Yellow fluorescent protein

INTRODUCTION

Brassica rapa pekinensis (abbreviated *B. rapa* hereafter), also called Chinese cabbage, is a common horticultural crop in East Asia. It is widely used in cuisine, and particularly important in Korea as the main ingredient of a traditional food "Kimchi". Known as a highly nutritious and healthy vegetable, Chinese cabbage has also become popular worldwide. Through breeding and cultivation improvement, people can get a good yield of Chinese cabbage, however, pests, bacterial and fungal diseases such as black rot, soft rot or blackleg, seriously impair its production. Bacterial soft rot is deemed one of the most destructive diseases that threaten *Brassica* species.

To defend themselves against pathogens, plants rely on their innate immune system where each individual cell can trigger local responses and produce systemic defense signals. Plant immunity is widely described as a multi-layered recognition system that involves transmembrane pattern recognition receptors (PRRs) and intracellular receptors **(Dodds and Rathjen, 2010; Dangl et al., 2013)**. PRRs perceive conserved pathogen-associated molecular patterns (PAMPs) and usually mediate profound and tractable defense responses called pattern-triggered immunity (PTI). PTI efficiently restricts the growth of pathogens and contribute to basal and durable disease resistance of plants. Adapted pathogens secrete virulence factors, termed effectors to interfere with PTI **(Dodds and Rathjen, 2010)**. However, those effectors can be perceived by intracellular receptors, which are also called resistance (R) proteins, containing nucleotide-binding (NB) and leucine-rich repeat (LRR) domains, and triggering a robust defense responses called effector-triggered

immunity (ETI). ETI is deemed commonly an accelerated and amplified responses of PTI, usually resulting in a hypersensitive response (HR) localized at the infection site **(Jones and Dangl, 2006)**. However, continued studies indicated that plant immune system is continuous and integrated, so it could not be narrowly defined using a simple PTI-ETI dichotomy **(Cook et al., 2015)**. PRRs are as dynamic as R proteins evolved via specific host-pathogen interaction. Both PRRs and PAMPs display dynamic variations even within a single species, suggesting a specific recognition rather than general perception **(Cook et al., 2015)**.

Well-characterized bacterial PAMPs include flagellin and its immunogenic epitope flg22 and flgII-28 **(Felix et al., 1999; Gómez-Gómez and Boller, 2000; Cai et al., 2011)**, elongation factor Tu (EF-Tu) and its epitope elf18 and EFa50 **(Kunze et al., 2004; Zipfel et al., 2006; Furukawa et al., 2014)**, cold shock proteins (CSP22) **(Felix and Boller, 2003)**, lipopolysaccharides (LPS) **(Erbs and Newman, 2012)** and a major component of bacterial cell walls, peptidoglycans (PGNs) **(Gust et al., 2007; Erbs et al., 2008)**. Likewise, the major component of fungal cell wall, chitin, is also a well described PAMP **(Shibuya and Minami, 2001)**. Little is known about the release of PAMPs that are usually embedded in the polymer structure. Recent study revealed that plant secreted β-galactosidase 1 (BGAL1) to release flagellin elicitor from glycosylated flagellin carrying a terminal modified viosamine, and plant-secreted proteases could process the deglycosylated flagellin to release the immunogenic peptide elicitors in the apoplast **(Buscaill et al., 2019)**. Significant variation exists in sequences of the same PAMP across microbe species that leads to diverse degrees of immune responses in plant, although PAMP is usually defined conserved because of its crucial and necessary role in the life of microbes. Likewise, the significant variation also exists in PAMP responsiveness among plant species or even within one plant species, resulting from the variation of PRR repertoire across

species or families.

Several PAMP responsive receptors PRRs have been identified, such as FLAGELLIN SENSITIVE 2 (FLS2), EF-TU RECEPTOR (EFR) or CHITIN ELICITOR RECEPTOR KINASE 1 (CERK1) **(Gómez-Gómez and Boller, 2000; Zipfel et al., 2006; Miya et al., 2007)**. PRRs identified so far are plasma membrane localized proteins in plant, and they are either receptor-like kinases (RLKs) or receptor-like proteins (RLPs). RLKs are composed of a ligand-binding ectodomain, a single pass transmembrane domain, and an intracellular kinase domain. RLPs share a similar structure with RLKs, but lack the kinase domain, suggesting that its full activation requires a cooperation with other kinase proteins. Relying on the ectodomains, PRRs could be also subdivided as leucine-rich repeats (LRR)-RLKs/RLPs that bind to proteins or peptides like flagellin and EF-Tu, lysine motifs (LysM)-RLKs/RLPs that bind to carbohydrate-based ligands like chitin and PGN, or lectin motifs (LEC)-RLKs/RLPs that bind to extracellular ATP or LPS **(Zipfel, 2014; Bohm et al., 2014)**. Neither RLKs nor RLPs could contribute PTI by themselves, they emanate and transduce the defense signals from the ectodomain after PAMP perception to activate the intracellular PTI pathway, relying on forming a PRR complexes with co-receptor or signal enhancer at the plasma membrane **(Monaghan and Zipfel, 2012; Macho and Zipfel., 2014)**. One of well-known co-receptor is BRI1-ASSOCIATED RECEPTOR KINASE 1 (BAK1), which is involved in flg22 or elf18 responsiveness through rapidly forming ligand-induced receptor complexes by heteromerization with FLS2 or EFR **(Chinchilla et al., 2007)**. Likewise, activation of CERK1 relies on the generation of PRR complex but independent of BAK1 **(Gimenez-Ibanez et al., 2009; Wan et al., 2008)**. The long chitin oligomers could lead *Arabidopsis* CERK1 (AtCERK1) to homodimerize into an active receptor complex **(Liu et al., 2012)**, whereas in rice, chitin-binding leads to the generation of

a multimeric receptor complex formed by OsCERK1 and the rice CHITIN ELICITOR BINDING PROTEINs (OsCEBiPs) **(Shimizu et al., 2010)**. To transmit defense signals and activate intracellular signaling cascades, receptor-like cytoplasmic kinases (RLCKs) play crucial roles as direct substrates of PRR complexes and positive regulators of PTI signaling **(Macho and Zipfel, 2014)**. One of best-studied examples is BOTRYTIS-INDUCED KINASE 1 (BIK1). Upon flg22 elicitation, BIK1 is rapidly phosphorylated by FLS2/BAK1 complex and activates downstream signaling components **(Zhang et al., 2010; Lu et al., 2010)**. Additionally, PBS1-LIKE KINASE (PBL) proteins, which belong to the same RLCK subfamily of BIK1 **(Zhang et al., 2010)**, are also important substrates of PRR complexes. Both are involved in not only flg22-triggered immunity but also elf18 or chitin-triggered immunity **(Zhang et al., 2010)**.

The downstream signaling of PRR complexes initiates a series of various PTI events, such as the expression of defense marker genes, reactive oxygen species (ROS) burst, ligand-induced endocytosis, etc.

Upon PAMP elicitation, selective transcriptional reprogramming is rapidly induced via the activation of mitogen-activated protein kinases (MAPKs) and calcium-dependent protein kinases (CDPKs) cascades by RLCKs **(Tena et al., 2011)**, resulting in the expression of immune responsive genes, such as genes correlated to PRR complexes or PTI signaling components. Interestingly, transcriptional reprogramming triggered by diverse PAMPs largely overlapped but with distinct temporal dynamics **(Li et al., 2016)**.

ROS burst is induced via the activation of NADPH oxidase by RLCK(s). For example, RESPIRATORY BURST OXIDASE HOMOLOG PROTEIN D (RBOHD) is directly phosphorylated by BIK1 and PBLs, resulting in ROS production in *Arabidopsis* **(Kadota et al., 2014; Li et al., 2014; Macho and Zipfel, 2014)**.

Ligand-induced endocytosis of PRR complexes is transiently stimulated after PAMP elicitation, suggesting a subcellular trafficking of PRRs and degradation of activated PRRs and non-self-patterns. PRR-mediated endocytosis seems to be dependent on PRR phosphorylation **(Robatzek et al., 2006)**. FLS2 internalization has been observed upon flg22 elicitation in *Arabidopsis* **(Robatzek et al., 2006)**. LPS of the phytopathogenic bacterium *Xanthomonas campestris* pv. *campestris* (X.c.c) could be internalized into the non-host plant cells of *Nicotiana tabacum* **(Gross et al., 2005)**.

Prolonged PAMP exposure inhibits plant growth, due to the trade-offs between growth and immunity. BAK1 is involved both in brassinosteroids (BR) pathway and PTI **(Li et al., 2002; Nam and Li, 2002; Chinchilla et al., 2007)**, most likely acting as a switch to balance these two pathways. However, BAK1 is not rate-limiting between BR and PTI pathways in native conditions, suggesting that the trade-offs between growth and defense is also in a BAK1-independent manner **(Albrecht et al., 2011)**. Seedling growth inhibition (SGI) of *Arabidopsis* Col-0 in response to flg22 has been observed in a dose-dependent manner **(Gómez-Gómez et al., 1999)**. Although the mechanism leading to SGI is still unclear, SGI is often used as a read-out of PTI to examine PAMP perception in plants.

PTI is deemed as slow, tractable and durable defense responses. However, continued studies showed that PAMPs or PRRs could induce cell death. Flagellin from *Pseudomonas avenae* or *Pseudomonas syringae* pv. *tabaci* could induce HR in nonhost rice or tomato cells, respectively **(Che et al., 2000; Marutani et al., 2005)**. And flagellin from *Pseudomonas syringae* pv. *tomato* could induce HR in tomato cells **(Taguchi et al., 2003)**. Moreover, a novel fungal PAMP called CELL DEATH INDUCING 1 (RcCDI1) which is identified in the *Rhynchosporium commune* transcript, as well as its homologues from other fungal species, could induce cell

death in *Nicotiana benthamiana* (*N. benthamiana*) **(Franco-Orozco et al., 2017)**. Intriguingly, overexpression of *AtCERK1* in *N. benthamiana* could induce cell death without PAMP elicitation **(Pietraszewska-Bogiel et al., 2013)**.

Although the intracellular signaling is largely conserved, the variation in PRR repertoire occurs across species and families. The best-studied PRRs, so far, are from the model plant *Arabidopsis thaliana* (*A. thaliana*). AtFLS2, which recognizes flg22 **(Gómez-Gómez and Boller, 2000)**, contains 28 LRRs ectodomain with direct flg22-binding sites **(Chinchilla et al., 2006; Dunning et al., 2007)**. Its homologs have been often found to be functional across species, for example in *N. benthamiana* **(Hann and Rathjen, 2007)**, in tomato **(Robatzek et al., 2007)** or in rice **(Takai et al., 2008)**, suggesting that flg22 is probably perceived by most higher plants. Unlike AtFLS2, AtEFR and its functional orthologs, which recognize elf18 **(Zipfel et al., 2006)**, has been found so far confined to the *Brassicaceae* family **(Kunze et al., 2004; Zipfel et al., 2006)**. Transient expression of *AtEFR* in *N. benthamiana* and transgenic expression of *AtEFR* in tomato, which both belongs to *Solanaceae* family, confers elf18 responsiveness **(Zipfel et al., 2006; Lacombe et al., 2010)**, indicating the expansion of PRR repertoire using interfamily transfer. In addition, PRR and its functional homolog(s) vary in structure across species. One of the best examples is CERK1 mentioned above. AtCERK1 contains three LysM domains and is able to directly bind to chitin oligomers **(Miya et al., 2007; Petutschnig et al., 2010; Liu et al., 2012)**, whereas its homolog OsCERK1 only has one single LysM domain and does not bind chitin oligomers directly by itself **(Shimizu et al., 2010)**.

B. rapa is closely related to *A. thaliana*. Both belong to *Brassicaceae* family and their lineages diverged from a common ancestor. Whole genome triplication occurred in Brassica **(Wang et al., 2011)**, resulting in the existence of duplicated or triplicated homologs of *A. thaliana* **(Force et al., 1999; Rastogi and Liberles, 2005)**.

Although PRRs and PTI signaling have been intensively investigated in *A. thaliana*, limited studies have been done to understand the defense system of Chinese cabbage. In order to decipher the molecular basis of PTI in Chinese cabbage, the range of PAMP responsiveness in Chinese cabbage was firstly investigated via assessing PTI typical responses. Secondly, comparative analysis revealed the presence of *BraPRR*s, the putative homolog(s) of *AtPRR*s, in *B. rapa* genome. Finally, putative *BraPRR*s candidates were cloned and characterized comparable to *AtPRR*s via transient expression in *N. benthamiana* and via functional complementation in transgenic *Arabidopsis prr* mutant. This study provided reliable tools to assess PAMP perception in Chinese cabbage, gave new insights into PRR repertoire of Chinese cabbage, and identified functional *B. rapa* homologs of *AtPRR*s, allowing to further test with new PAMPs, and helping to design strategies to construct batter arsenal of plant against pathogens and finally to improve the production of Chinese cabbage.

MATERIALS AND METHODS

Plant materials and growth conditions

Chinese cabbage (*Brassica rapa* spp. *pekinensis*) seeds were provided from Hungnong company in Korea. The commercial name was Norang Kimchi Baechu. Chinese cabbage seeds were sown in the soil (BioGreen), then germinated and grown at 23 °C and 60% humidity in a 10 h light/14h dark cycle (short-day condition, SD condition) in an environment-controlled chamber.

 Nicotiana benthamiana seeds were sown in the soil (BioGreen), transferred 2 weeks after sowing and grown at 24 °C and 60% humidity in a 16 h light/8h dark cycle (long-day condition, LD condition) in an environment-controlled room.

 Arabidopsis thaliana seeds of wild-type (WT) Columbia (Col-0), *fls2* single mutant, and *fls2 efr cerk1* (*fec*) triple mutant were provided from Plant immunity laboratory at Pohang University of Science and Technology (POSTECH). *fls2* (SALK_093905, T-DNA insertion in the first exon) and *fec* mutants were generated from the Col-0 background, described in previous studies **(Heese et al., 2007, Gimenez-Ibanez et al., 2009)**. All *A. thaliana* seeds were vernalized at least for 4 days at 4 °C, and sown in the soil (BioGreen) or in Murashige and Skoog (MS) medium. Plants were germinated and grown at 23 °C and 60% humidity 1) in a 10 h light/14h dark cycle in an environment-controlled chamber for ROS burst measurement or 2) in a 16 h light/8h dark cycle in an environment-controlled room for SGI assay and for generation of *PRR* -transgenic lines.

PAMP solutions

Flg22 (flg22-Pto, QRLSTGSRINSAKDDAAGLQIA, **Felix et al., 1999**), elf18 (Ac-SKEKFERTKPHVNVGTIG, **Kunze et al., 2004**) and CSP22 (CSP22-Rsol, ATGTVKWFNETKGFGFITPDGG) peptides were synthesized by Peptron company. flgII-28 (flgII-28-Pto, ESTNILQRMRELAVQSRNDSNSSTDRDA) was synthesized by GL Biochem (Shanghai) Ltd. Four peptides were resuspended in sterile H_2O at 10 mM and were divided into 10 µM then stored at -20 °C. Chitin (GlcNac)$_7$ from crab shells was provided from Sigma-Aldrich company. Chitin products were resuspended in sterile H_2O at 10 mg/mL and autoclaved before storing at -20 °C. LPS and PGN products were provided by Kyeong- Ho Won, RDA, Naju. LPS were resuspended in sterile H_2O at 5 mg/mL and PGN at 10 mg/mL then stored at -20 °C.

RNA isolation and cDNA synthesis

To detect defense marker gene expression **[Figure 1]**, 6 leaf discs (diameter = 5 mm) were collected with a cork borer and recovered on 1000 µL of sterile H_2O overnight. Then leaf discs were challenged with water or PAMP for 30 min, 60 min or 180 min, then rapidly frozen in liquid nitrogen. To measure *BraPRR*-expression level **[Figure 4]**, leaf materials with a weight equal to 6 leaf discs (diameter = 5 mm) were collected with a cork borer or scissor and rapidly frozen in liquid nitrogen. And to monitor transgene-expression **[Figure 11]**, plant material of transgenic *EFR* expressing lines was collected from four seedlings, which were 14-day-old, germinated and grown on solid MS medium for 4 days and grown in liquid MS medium for additional 10 days. The material of transgenic *FLS2* and *CERK1* expressing lines was collected in

the way followed: 1 leaf disc (diameter = 5 mm) per plant was collected with a cork borer from eight different 5-week-old plants, total of 8 discs per line were rapidly frozen in liquid nitrogen.

Total RNA was isolated using TRIzol-Reagent (Ambion) and treated with DNase I (Sigma-Aldrich) for genomic DNA (gDNA) digestion.

1.5 µg isolated RNA was used for cDNA synthesis using Maxima cDNA synthesis kit (Thermo Fisher Scientific). Reverse Transcription (RT) protocol was programed as following: 25 °C 10 min, 50 °C 30 min, 85 °C 5 min. Cover temperature was 105 °C and total reactive volume was 20 µL.

Synthesized cDNA was diluted 5 times and 1 µL was used as template in Reverse transcription polymerase chain reaction (RT-PCR) and Quantitative Real-time PCR (qPCR or qRT-PCR) process.

Reverse transcription polymerase chain reaction (RT-PCR)

RT-PCR products were amplified using Prime taq (GeNetBio, Korea). The primers are listed in **Appendix A**. The RT-PCR reaction was performed in 20 µL and heated for 1 cycle of 5 min at 95 °C (Stage I), 20 to 35 cycles of 30 sec at 95 °C, 30 sec at 55 to 60 °C and 30 to 40 sec at 72 °C (Stage II), and 1 cycle of 7 min at 72 °C and 5 min at 25 °C (Stage III).

Quantitative Real-time PCR (qRT-PCR or qPCR)

qRT-PCR was performed with Roche LightCycler 480 using GoTaq qPCR master mix (Promega). The primers are listed in **Appendix A**. The qRT-PCR reaction was performed in 20 µL under the detection format of SyBR Green I/HRM Dye heated

for 1 cycle of 5 min at 95 °C (Stage I), 45 cycles of 10 sec at 95 °C, 10 sec at 58 to 60 °C, and 10 to 40 sec at 72 °C with signal detection (Stage II: Quantification), and was followed by a stage of melting curve analysis of 5 sec at 95 °C, 30 sec at 65 °C and continuous at 97 °C, and finally a dissociation stage of 30 sec at 40 °C.

Data was analyzed using program Conversion LC480 and LinRegPCR.

Oxidative burst measurement

Leaf discs (diameter = 5 mm) were collected with a cork borer and recovered on 150 µL of sterile H_2O overnight. 16 h after collecting, the water was removed and leaf discs were challenged with a solution of 100 µM luminol (Sigma-Aldrich) and 2 µg/µL horseradish peroxydase (Sigma-Aldrich) containing PAMPs. The amount of relative light unit (RLU) was measured over a period of 75 or 114 min using GloMax 96 Microplate Luminometer (Promega).

Cloning and Construction of *PRR* library

PRR genes were cloned using Golden Gate Assembly technology **[Figure 5]**. Gene of interest was divided into three to four ~1 kb modules. Each module was amplified using Phusion High-Fidelity DNA polymerase (Thermo Fisher Scientific) by RT-PCR. The primers used for amplifying each module are listed in **Appendix A**. PCR products were resolved on 1% agarose. Band of interest was purified through gel extraction and ligated into the cloning vector pICH41021 (pUC19B) by *Sma*I/T4 ligase (Both from New England BioLabs). After sepharose-purification, the cloning constructs were transformed to *E. coli* strain DH5α using electroporation. After culture and selection on LB plate containing antibiotic ampicillin or carbenicillin and

X-gal/IPTG overnight, white single colonies were picked and cultured in liquid LB containing antibiotic ampicillin or carbenicillin overnight. Plasmid DNA of cultured cells was extracted by Miniprep then confirmed by *Bsa*I-digestion and by sequencing method. The *E. coli* strain DH5α carrying confirmed cloning-construct of modules were stored at -80°C.

To assemble all modules into final construct and fuse with 6xHA or YFP tag, all plasmids carrying the module-construct, backbone vector pICH86988 and vector carrying 6xHA or YFP-tag were added to set up assembly reaction with *Bsa*I/T4 DNA ligase (Both from New England BioLabs). The assembly reaction was heated for 25 cycles of 3 min at 37 °C and 4 min at 16 °C (Stage I), and 1 cycle of 5 min at 50 °C, 5 min at 80 °C and 5 min at 20 °C (Stage II).

The final constructions were confirmed by restriction digest and transformed into *Agrobacterium tumefaciens* (*A. tumefaciens*) strain AGL1 using electroporation. After culture and selection on LB plate containing antibiotic carbenicillin and kanamycin, one white single colony was picked to culture in liquid LB containing antibiotic carbenicillin and kanamycin overnight and stored at -80 °C as cell stock.

Point mutations of *PRR* kinase dead version were generated using site-directed mutagenesis by RT-PCR. The primers used in mutagenesis are listed in **Appendix A**. The mutagenesis reaction was heated for 1 cycle of 1 min at 95 °C (Stage I), 15 cycles of 50 sec at 95 °C, 1 min at 55 °C and 4 min at 72 °C (Stage II), and 1 cycle of 10 min at 68 °C, and 5 min at 20 °C (Stage III).

PCR product of mutagenesis was digested by *Dpn*I for 1 to 2 h and resolved on 1% agarose with PCR product without digestion as a control to confirm mutant strand synthesis. After sepharose-purification, the construct of mutagenesis was transformed to *E. coli* strain DH5α using electroporation. Plasmid DNA extracted using Miniprep was confirmed by restriction digest and by sequencing.

All the constructs in this study are listed in **Appendix B**.

Agrobacterium-mediated transient expression in *N. benthamiana*

A. tumefaciens strain AGL1 cells carrying the expression vector were grown in LB medium containing antibiotic carbenicillin and kanamycin overnight. After spinning down, the cells were resuspended in buffer (10 mM $MgCl_2$ and 10 mM MES-KOH, pH=5.6) and adjusted the suspension to OD_{600}=0.004 to 0.5. Adjusted bacterial suspension was pressure infiltrated into 5 or 6-week-old *N. benthamiana* leaves with a needleless syringe.

Subcellular localization analysis

2 days after infiltration, leaf discs (diameter = 8 mm) of *N. benthamiana* transformed by *A. tumefaciens* strain AGL1 cells carrying the expression vector were collected with a cork borer and rinsed in sterile water, 1 M NaCl or 100 nM flg22 before imaging. Imaging was performed using Confocal Laser Scanning Microscope (Leica SP8 X). Fluorescence analysis was done with a 20x or 40x water lens objective under White Light Laser (WLL, 470 – 670 nm, 1 nm tunable laser). YFP fluorescence was collected with 514 nm excitation wavelength and 527 nm emission wavelength. GFP fluorescence was collected with 489 nm excitation wavelength and 509 nm emission wavelength.

Generation of transgenic *PRR* expressing lines

To generate transgenic *PRR* expressing lines, *Arabidopsis* background plant was transformed with *A. tumefaciens* strain AGL1 carrying insert gene construct using floral dip method **(Clough and Bent, 1998)**. The information of insert gene construct and *Arabidopsis* background plant is listed in **Appendix B**. Transformant-seeds generated from self-pollination of previous generation plants which were screened on MS medium containing antibiotic kanamycin. The amount of surviving T1 plants, the segregation ratio of T2 plant and selected T3 homozygous lines (100% resistance) are listed in **Appendix C**.

PAMP-triggered seedling growth inhibition

Seeds were stored at 4 °C. To sow on MS medium, seeds were sterilized with solution I (0.05% Triton X-100 and 70% ethanol) twice and solution II (95% ethanol) once. After drying on sterile paper, seeds were sown on solid MS medium and grown at 23 °C and 60% humidity in a 16 h light/8h dark cycle in an environment-controlled room. 4 days after sowing, seedlings were transferred to 24-well plates. Each well was filled with 990 µL of liquid MS medium and 10 µL of H_2O or PAMP solutions. 2 seedlings were transferred per well. 24-well plates were kept in same condition. 2 weeks after sowing, fresh weight of seedling was measured using high precision digital balance.

RESULTS

Pattern-triggered immune responses in Chinese cabbage

Multiple homologs of AtPRRs exist in Chinese cabbage genome.

In order to predict PRR repertoire of Chinese cabbage, the putative *PRR*s were primarily sought in Chinese cabbage genome. Although it was difficult to find a database that describes the exact genetic data of *B. rapa* hybrid cultivar line "Norang kimchi baechu" which is used in this study, the *Brassica* database (BRAD) provides the complete *Brassica* 'A' genome sequence from *B. rapa* cultivar line "Chiifu-401" **(Cheng et al., 2011)**.

Using BRAD, multiple homologs of known *Arabidopsis PRR*s (*AtPRR*s) were found in *B. rapa* genome. Two *B. rapa* genes were syntenic orthologs of *A. thaliana EFR, FLS2* and *LYM1*, respectively. One was syntenic ortholog of *CERK1* and *LYM3*, individually. Besides, one *B. rapa* gene was a non-syntenic ortholog of *LORE*. However, *CORE, CSPR, FLS3*, which are known so far only to be confined to the *Solanaceae* family, no homolog of them could be found in Chinese cabbage genome. Furthermore, at least 72.2 % amino acid residues were identical between the protein sequences of *B. rapa* homologs to their orthologs in *A. thaliana* **[Table 1]**, suggesting highly structural similarity and high conservation between AtPRRs and their homologous PRRs in *B. rapa* (BraPRRs). Hence, Chinese cabbage seems to possess receptors to detect chitin, elf18, flg22, LPS and PGN but could not respond to CSP22 and flgII-28.

Table 1 | Homologs of known *PRR*s in *B. rapa* genome

Gene	Pattern (ligand)	Gene ID	Receptor Family	Reference	*B.rapa* homolog[a]	Gene fractionation[a]	A.A identity
CERK1	N-acetylglucosamine (chitin)	AT3G21630	LysM-RLK	Miya et al. (2007)	Bra031293 (s)	LF	83.5%
CORE	Cold shock protein (CSP22)	Solyc03g096190	LRR-RLK	Wang et al. (2016)	-		
CSPR	Cold shock protein (CSP22)	Niben101Scf03240g00007	LRR-RLP	Saur et al. (2016)	-		
EFR	Elongation factor Tu (elf18)	AT5G20480	LRR-RLK	Zipfel et al. (2006)	Bra002305 (s)	LF	76.7%
					Bra006560 (s)	MF1	78.2%
FLS2	Flagellin (flg22)	AT5G46330	LRR-RLK	Gómez-Gómez et al. (2000)	Bra017563 (s)	MF2	73.7%
					Bra022032 (s)	MF1	72.2%
FLS3	Flagellin (flgII-28)	Soly04g009640	LRR-RLK	Hind et al. (2016)	-		
LORE	Lipopolysaccharides (LPS)	AT1G61380	LEC-RLK	Ranf et al. (2015)	Bra027088		75.0%
LYM1	Peptidoglycan (PGN)	AT1G21880	LysM-RLP	Willmann et al. (2011)	Bra016402 (s)	MF1	86.6%
					Bra017956 (s)	LF	87.1%
LYM3	Peptidoglycan (PGN)	AT1G77630	LysM-RLP	Willmann et al. (2011)	Bra008320 (s)	MF1	79.7%

[a] From *Brassica* database (BRAD) http://brassicadb.org

(s): syntenic gene

-: absence

LF: Less Fractioned subgenome

MF1: Moderate Fractioned subgenome

MF2: Most Fractioned subgenome

AA: Amino Acid residues

PAMPs upregulated the expression of defense marker genes in Chinese cabbage.

PAMP perception leads to PTI events in plant. Early PTI events include selective transcriptional reprogramming and rapid ROS burst. To confirm the hypothesis above about PAMP-perception of Chinese cabbage and predict the function of BraPRRs, selective transcriptional reprogramming was assessed through detecting the regulation of PAMP-induced marker gene expression in Chinese cabbage.

First, it required to identify a reliable marker gene whose expression could significantly and rapidly induced by several PAMPs. Because of the conserved downstream of PRRs in plant cells, the homologs of *Arabidopsis* marker genes were often found implement as effective markers in other species. Although *B. rapa* and A. *thaliana* are genetically close, it was still required to validate the homologs of *Arabidopsis* marker genes in Chinese cabbage. The *B. rapa* genes, which are orthologous to *Arabidopsis* defense marker gene *AtNHL10*, *AtCYP81F2*, *AtMPK4* and *AtWRKY33*, were selected as the candidates. And flg22, which is perceived by most higher plants, was chosen as an elicitor. Chinese cabbage discs were exposed to 100 nM flg22 for 1 h and 3 h. flg22 exposure resulted in the upregulation within 1 h and downregulation within 3 h of all marker gene candidates compared to the control with water (H_2O) treatment. Among them, the expression level of *BraNHL10* and *BraCYP81F2* were significantly low upon water (H_2O) treatment **[Figure 1A]**, therefore these two candidates were selected to identify whether they were reliable in response to several PAMPs. Either *BraNHL10* or *BraCYP81F2* was consistently upregulated following 1 h treatment with flg22, elf18, chitin, CSP22 and LPS in Chinese cabbage leaves **[Figure 1B]**. Two marker genes were strongly induced in response to chitin. Relatively, upon PGN-treatment, it was difficult to define the

change of *BraNHL10* and *BraCYP81F2* gene expression compared to water treatment **[Figure 1B]**. So far, *BraNHL10* and *BraCYP81F2* were both effective marker genes for PAMP-responsiveness. Here *BraNHL10* was selected for following kinetic study.

To describe the kinetics of defense gene expression, Chinese cabbage discs were treated with water, 100 nM flg22, 100 nM elf18, 100 µg/mL chitin, 100 nM CSP22, 50 µg/mL LPS, 100 µg/mL PGN and 100 nM flgII-28 for 30 min, 1 h or 3 h. *BraNHL10* expression was strongly upregulated within 30 min in response to flg22, elf18 and chitin and downregulated at 1 h, and finally returned to background level at 3 h time point **[Figure 1C]**. In response to CSP22 and LPS, *BraNHL10* expression was slightly upregulated within 30 min. After 30 min, *BraNHL10* expression was downregulated upon CSP22 elicitation, however, slightly and continuously upregulated in response to LPS. In addition, in response to PGN and flgII-28, *BraNHL10* expression level was too low to be visible in agarose gel, comparable to water-treatment control **[Figure 1C]**. Therefore, flg22, elf18 and chitin apparently induced the expression of defense marker gene *BraNHL10* in Chinese cabbage. And Chinese cabbage seemed to perceive CSP22 and LPS, but probably could not recognize PGN and flgII-28.

Consistent with the kinetic results observed by semi-quantitative PCR, quantitative analysis showed *BraNHL10* expression was upregulated 43-fold in response to 100 nM flg22, 19-fold in response to 100 nM elf18, 47-fold in response to 100 µg/mL chitin and 2-fold in response to 100 nM CSP22 within 30 min and reduced between 30 min to 1 h then recovered to background level after 3 h compared to H_2O treatment **[Figure 1D]**. Among four PAMPs, *BraNHL10* expression was strongly induced in response to chitin (47-fold) and flg22 (43-fold) and the expression maintained at a considerable level, 42-fold upon chitin treatment

and 32-fold upon flg22 treatment, at 1 h. Conversely, *BraNHL10* expression in response to elf18 was strongly downregulated to 2-fold at 1 h. With water-treatment, although a slight reduction of *BraNHL10* expression was observed at 3 h, the change was insignificant to the expression level at 30 min or at 1 h, and it was significantly lower than other treatments **[Figure 1D]**. Here the existence of flg22, elf18 and chitin sensing PRRs in Chinese cabbage could be subsequently hypothesized. Flg22, elf18 and chitin were selected as the elicitors and their responsive receptors were focused to decipher in further study.
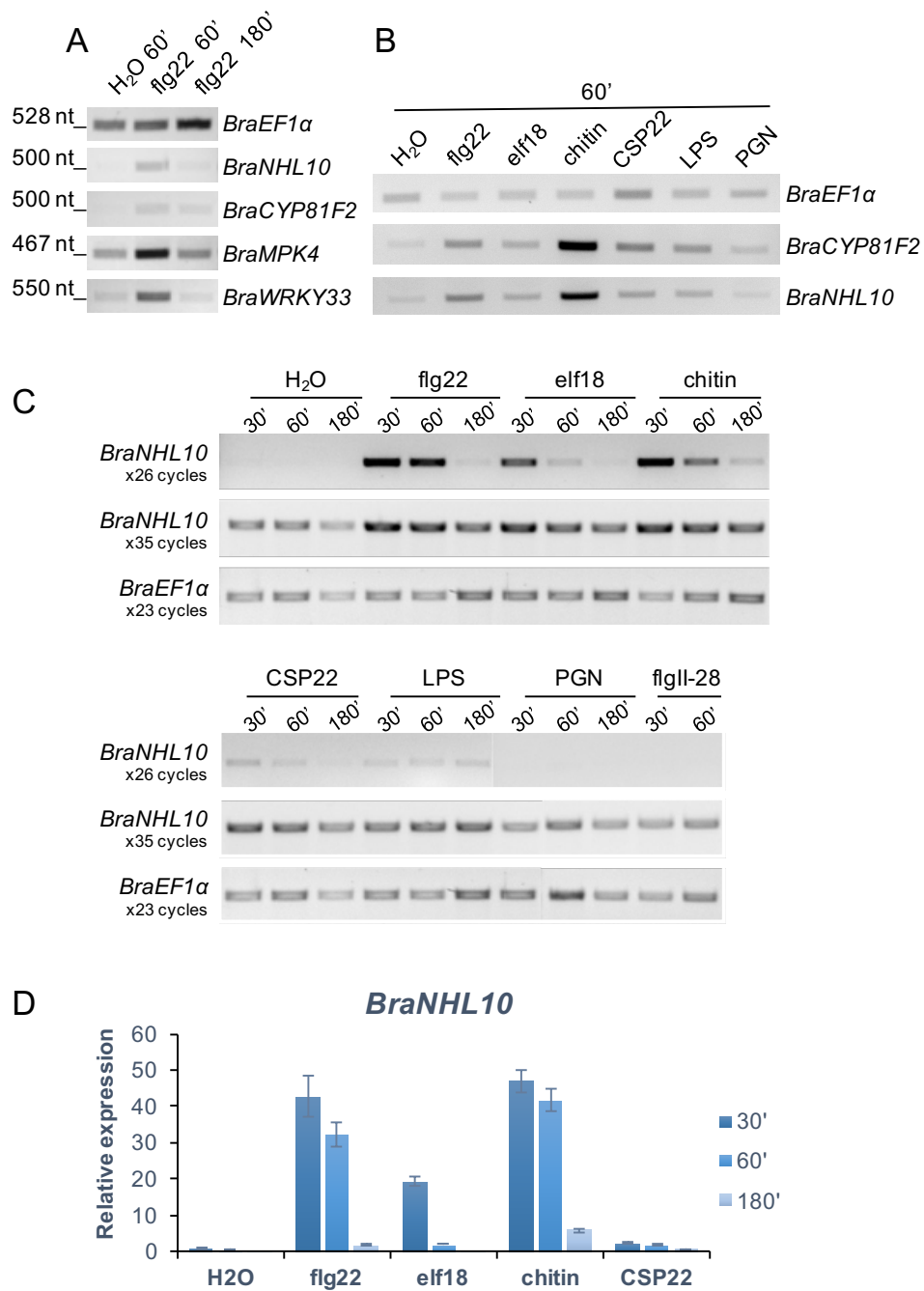
Figure 1 | PAMP-responsive defense marker gene expression

5-week-old Chinese cabbage leaf discs were challenged with water (H_2O) or PAMPs for 30 minutes, one hour or three hours before RNA extraction. Concentrations of PAMPs were 100 nM flg22, 100 nM elf18, 100 µg/mL chitin, 100 nM CSP22, 50 µg/mL LPS, 100 µg/mL PGN and 100 nM flgII-28. **(A)**, **(B)** and **(C)** Housekeeping gene *BraEF1α* and Marker genes (*BraNHL10, BraCYP81F2, BraMPK4* and *BraWRKY33*) were amplified by RT-PCR. RT-PCR products were resolved on 1.5% agarose. **(D)** PAMP-induced *BraNHL10* gene expression was monitored by qRT-PCR. Expression level was normalized against *BraEF1α* gene expression. The expression level of *BraNHL10* in the sample with H_2O-treatment for 30 minutes assigned the value 1. Values are presented as mean of the relative *BraNHL10* expression level in three technical replicates ± standard error. Representative data from one of three biological repeats are presented.

flg22, elf18 and chitin triggered ROS burst in Chinese cabbage.

ROS burst is one of the typical early immune responses mediated by NADPH oxidases localized at the plasma membrane in plant, and it is well-known as a subsequent event of PRR complexes-activation upon PAMP-perception. ROS are usually generated within a few minutes after PAMP treatment. Using a luminol-based assay, ROS burst could be detected in laboratory. To further examine flg22, elf18 and chitin responsiveness in Chinese cabbage, ROS burst was analyzed in Chinese cabbage and *A. thaliana* wild-type plant Col-0. Leaf discs were exposed in a series concentration gradient of flg22, elf18 (1 nM, 10 nM, 100 nM or 1000 nM) or chitin (10 µg/mL, 100 µg/mL or 1000 µg/mL). As shown in results, water treatment did not cause a significant change of ROS production. Increasing the dose of PAMPs, ROS was produced faster and with larger amplitudes within approximately 50 min, indicating that flg22, elf18 and chitin trigger ROS burst in kinetic and dose-dependent manner. And slight differences in the amplitude and saturation could be observed between the responses of *B. rapa* and *A. thaliana* **[Figure 2]**.

In response to flg22, Chinese cabbage produced ROS earliest and accumulated ROS earliest to the maximum peak after 1000 nM treatment **[Figure 2A flg22]**. Along with dose increase, ROS production was induced faster and reached the maximum peak earlier. Total ROS production was also significantly accumulated with concentration gradient increased from 1 nM to 100 nM and saturated with 100 nM **[Figure 2B flg22]**. However, the concentration gradient did not affect the period of recovery back to background level except with 1 nM **[Figure 2A flg22]**. With 1 nM treatment, ROS was induced within 10 min. The ROS induction was delayed compared to the induction within 3 min with other concentration. The ROS production finished within approximately 39 min earlier than 55 min with other

concentration. Compared to Chinese cabbage, ROS burst was rarely observed with 1 nM treatment in Col-0. And unlike the kinetic behaviors which were similar between 100 nM and 1000 nM in Chinese cabbage, ROS production upon 100 nM treatment in Col-0 increased and decreased more slowly than with 1000 nM **[Figure 2A flg22]**, leading to a higher total ROS production with 100 nM than with 1000 nM although the difference was insignificant **[Figure 2B flg22]**. Furthermore, ROS production with 1000 nM treatment in Col-0 reached the maximum peak approximately 3 min earlier than Chinese cabbage. All ROS production of Col-0 in this assay finished approximately 8 min earlier than Chinese cabbage **[Figure 2A flg22]**. In addition, total ROS production of Chinese cabbage was approximately 2 to 5 times more than Col-0 compared to the same concentration between two species **[Figure 2B flg22]**.

In response to elf18, ROS production saturated with 10 nM treatment in Chinese cabbage, the kinetics behaved similar with 10 nM, 100 nM and 1000 nM although the maximum value was sequentially raised **[Figure 2A&B elf18]**. With 1 nM treatment, total production was significantly reduced compared to 10 nM **[Figure 2B elf18]**and the induction was also delayed 5 min, however, there was no delay for the recovery **[Figure 2A elf18]**. Same as with other treatments, it recovered to background level within 33 min. Compared to the consistent behaviors in Chinese cabbage, the induction of ROS burst in Col-0 was apparently delayed with concentration gradient decreased. ROS burst with 1000 nM treatment in Col-0 was induced earliest but recovered to background level fastest **[Figure 2A elf18]**. This behavior led to reduce total ROS production less than with 100 nM, 10 nM and 1 nM **[Figure 2B elf18]**. ROS production reached the highest maximum peak and saturated with 10 nM **[Figure 2A&B elf18]**. Unlike in Chinese cabbage, ROS responded significantly strongly to 1 nM treatment in Col-0. ROS induced earlier

and the duration of response was longer in Col-0 than in Chinese cabbage **[Figure 2A elf18]**. Total ROS production in Col-0 was approximately 6 to 10 times more than in Chinese cabbage compared to the same concentration between two species **[Figure 2B elf18]**.

In response to chitin, ROS burst in Chinese cabbage was induced early and simultaneously within approximately 1 min with 100 and 1000 μg/mL treatment **[Figure 2A chitin]**. But ROS burst reached the maximum peak within approximately 7 min and saturated with 100 μg/mL **[Figure 2A&B chitin]**. With 1000 μg/mL, ROS burst reached the maximum peak within approximately 16 min with a little higher value than with 100 μg/mL **[Figure 2A chitin]**. ROS burst is slightly induced with 10 μg/mL but rarely shown in kinetic figure and the total production was insignificantly different to water control **[Figure 2A&B chitin]**. Compared to Chinese cabbage, Col-0 generated ROS within 3 min a little later than Chinese cabbage and the maximum value was decreased significantly along with concentration gradient decrease, leading to constant decreases of total production in a dose-dependent manner **[Figure 2A&B chitin]**. Total ROS production of Col-0 was higher than Chinese cabbage only with 1000 μg/mL condition. With 100 μg/mL, the total production in Col-0 was only half of Chinese cabbage **[Figure 2B chitin]**. However, Col-0 showed a long and durable ROS response upon chitin elicitation **[Figure 2A chitin]**.

Compared between flg22, elf18 and chitin, flg22 seems to be the most effective elicitor to ROS response in Chinese cabbage, and Chinese cabbage seems to be more sensitive than Col-0 in response to flg22. Hence, feasible molecular tools had been obtained to measure PTI signaling in Chinese cabbage, and all results indicated that Chinese cabbage can perceive major PAMPs and trigger defense responses.
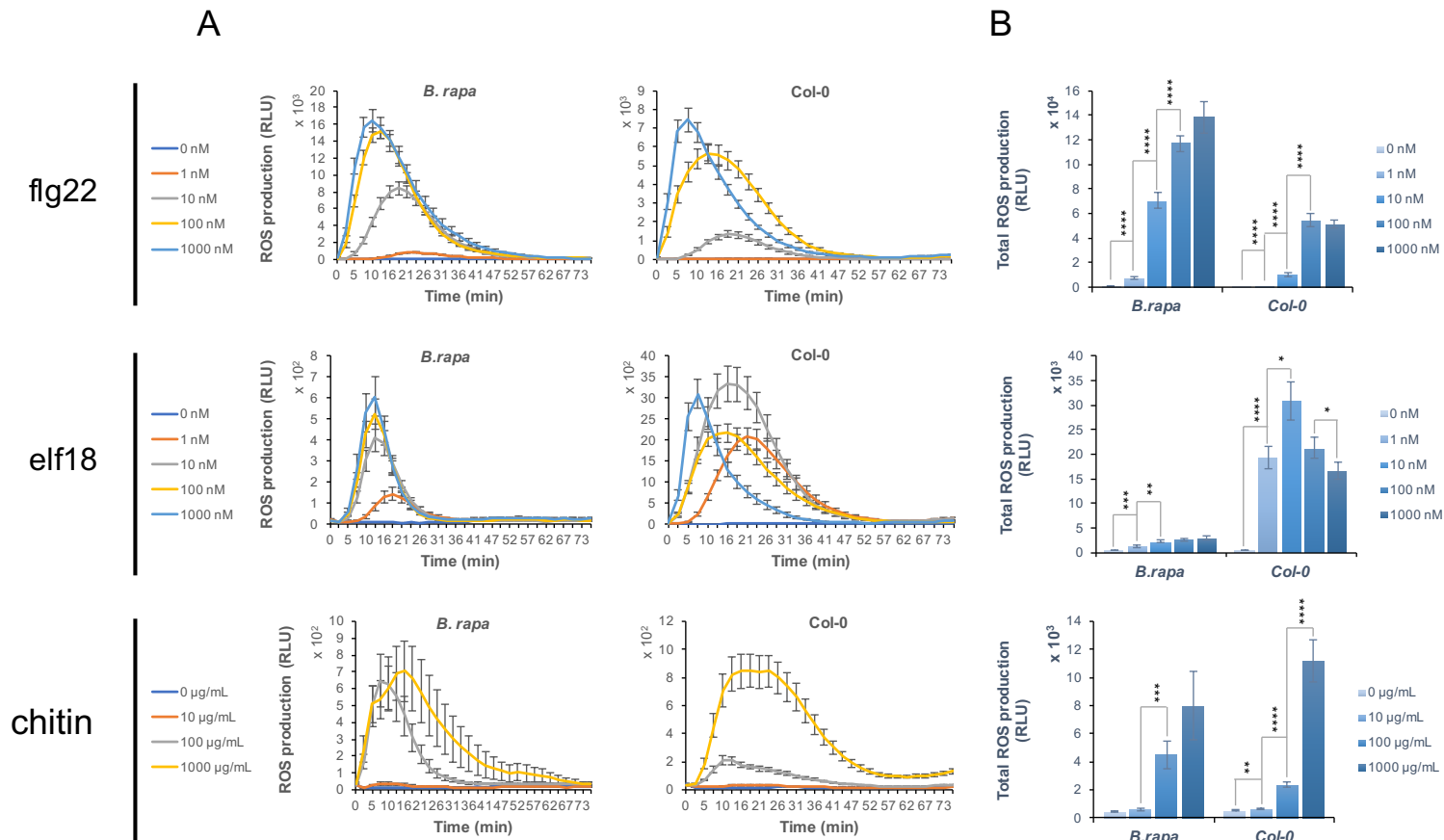
Figure 2 | PAMP-induced ROS production in *B.rapa* and *A.thaliana* Col-0

6-week-old Chinese cabbage and Col-0 leaves were challenged with different concentrations of flg22, elf18 (1 nM, 10 nM, 100 nM and 1000 nM) or chitin (10 µg/mL, 100 µg/mL and 1000 µg/mL). For each condition, 16 to 24 leaf discs were collected. ROS production (Relative Light Unit) was measured by chemiluminescence of oxidized luminol. **(A)** Kinetic and **(B)** total ROS production was measured for 75 minutes in three biological replicates ± standard error. Asterisks indicate significant differences between each concentration compared by Student's T-test. ****: $p < 0.0001$ ***: $0.0001 < p < 0.001$ **: $0.001 < p < 0.01$ *: $0.01 < p < 0.05$ ns: $p \geq 0.05$.

Identification and characterization of *BraFLS2*, *BraEFR* and *BraCERK1* candidates

At least one B. rapa ortholog of AtFLS2, AtEFR and AtCERK1 express in Chinese cabbage.

According to flg22, elf18 and chitin-induced marker gene *BraNHL10* expression and ROS burst, the existence of BraFLS2, BraEFR and BraCERK1 could be subsequently hypothesized. Ortholog of known PRR was often found functional in other species. The genes found in *B. rapa* accession Chiifu-402-42, which are orthologous to AtFLS2, AtEFR and AtCERK1 **[Table 1]**, were considered as *BraPRR* candidates. Firstly, the expression level of *FLS2* candidates (*BraFLS2*), *EFR* candidates (*BraEFR*) and *CERK1* candidate (*BraCERK1*) was extracted from published analysis of Chinese cabbage tissue-specific transcriptome **(Tong et al., 2013) [Table 2]**. Among *BraFLS2* candidates, only Bra017563 was expressed in *B. rapa* organs, and there were no reads mapped to Bra022032, indicating that Bra022032 was most likely unexpressed. Two of *EFR* candidates, Bra002305 and Bra006560 were expressed in *B. rapa* organs but at a low level, especially Bra006560. *CERK1* candidate Bra031293 is expressed at a relatively high level in *B. rapa* organs **[Table 2]**.

Table 2 | Expression of *BraFLS2, BraEFR* and *BraCERK1* in *B.rapa* organs

Gene	*B. rapa* orthologs	Root_1	Root_2	Stem	Leaf_1	Leaf_2	Flower	Silique	Callus
FLS2	Bra017563	4.41	4.77	4.51	6.12	5.83	2.23	2.05	4.52
	Bra022032	0.00	0.00	0.00	0.00	0.00	0.00	0.00	0.00
EFR	Bra002305	1.31	1.27	0.38	0.97	1.02	0.14	0.30	0.82
	Bra006560	0.31	0.14	0.11	0.29	0.11	0.03	0.00	0.15
CERK1	Bra031293	8.06	8.34	4.43	4.62	4.48	4.09	2.59	6.66

Data extracted from Cheng et al., 2011 and Tong et al., 2013.

FPKM: Fragments per kilobase of exon per million fragments mapped

BraPRRs share a high similarity with their orthologous AtPRRs in protein sequences.

To decipher whether the slight difference of immune responses in the oxidative burst assay between Chinese cabbage and Col-0 could be relevant to the degree of similarity in protein sequences, the protein sequences of BraPRRs and their orthologous AtPRRs were aligned using Geneious 10.2.6 and manually annotated the functional domains referring to UniProt.

For expressed gene BraFLS2 (Bra017563), the gene sequence was shorter than the previous one sought in BRAD database. The new annotated protein sequence shared 80% A.A identity with AtFLS2 **[Table 3A]**, higher than 73.7% with old annotations shown in **Table 1**. All functional domains in AtFLS2 could be found in Bra017563 **[Figure 3A]**, whereas the other unexpressed BraFLS2 (Bra022032) were difficult to find LRR17, 18 and 19 domains by alignment. In addition, the first flg22-binding site which corresponds to tyrosine (Y148) in AtFLS2 was shown mutated in BraFLS2 (Bra022032). And the protein of Bra022032 missed 2 amino acids in the end of helical transmembrane region corresponsive to leucine (L826) and isoleucine (I827) in AtFLS2 **[Figure 3B]**. Furthermore, BraFLS2 (Bra017563) shared 80.4% identity in LRR domains and 83.2% in kinase domain with those domains of AtFLS2. BraFLS2 (Bra022032) shared 71.9% in LRR domains and 72.8% in kinase domain with those of AtFLS2 **[Table 3A]**. BraFLS2 (Bra017563) shared higher identity in LRR domains and in kinase domain with those domains of AtFLS2 than BraFLS2 (Bra022032), indicating that Bra017563 was probably the functional *BraFLS2* gene.

Compared two BraEFRs, the protein of lower expressed Bra006560 shared, however, a little higher A.A identity (78.2%) with AtEFR than the protein translated from Bra002305 (76.7%) **[Table 3B]**. And Bra006560 also shared a little higher

identity in LRR domains (78.2%) and in kinase domain (83.2%) with those in AtEFR, compared to Bra002305 **[Table 3B]**. All functional domains between two BraEFR proteins seemed to be similar except signal peptide (SP) domain and transmembrane (TM) domain. In SP domain, protein of Bra002305 shared only 29.2% identity with AtEFR, very low compared to 60% of Bra006560 protein. On the contrary, in TM domain, protein of Bra006560 shared only 55.0% identity with AtEFR whereas protein of Bra002305 shared 81.0% **[Table 3B]**. Neither Bra002305 nor Bra006560 lost functional domain examined by annotation **[Figure 3C&3D]** and the protein sequences of two BraEFRs were very similar, sharing 75.0% A.A identity **(data not shown)**. It was difficult to infer the reason of low expression level of Bra006560 upon protein sequence, and was difficult to confirm which candidate functions in Chinese cabbage, one or both.

At last, BraCERK1 (Bra031293) shared 83.5% of high A.A identity with AtCERK1, all functional domains were highly similar to AtCERK1 except SP domain with 50.0% of identity. Especially, the kinase domain of BraCERK1 showed be highly conserved in the evolution, sharing 95.6% of similarity with AtCERK1 **[Table 3C]**. Every functional domain could be found corresponsive to those in AtCERK1 **[Figure 3E]**, indicating Bra031293 most likely functions as *BraCERK1* in Chinese cabbage.

Score = 4774.0, Identities = 941/1176 (80%), Positives = 1042/1176 (88%), Gaps = 5/1176 (0%)

B

Score = 4036.0, Identities = 845/1179 (71%), Positives = 962/1179 (81%), Gaps = 78/1179 (6%)

C

Score = 4052.0, Identities = 796/1042 (76%), Positives = 901/1042 (86%), Gaps = 22/1042 (2%)

Score = 4107.0, Identities = 809/1038 (77%), Positives = 895/1038 (86%), Gaps = 13/1038 (1%)

E Score = 2618.0, Identities = 518/620 (83%), Positives = 555/620 (89%), Gaps = 7/620 (1%)
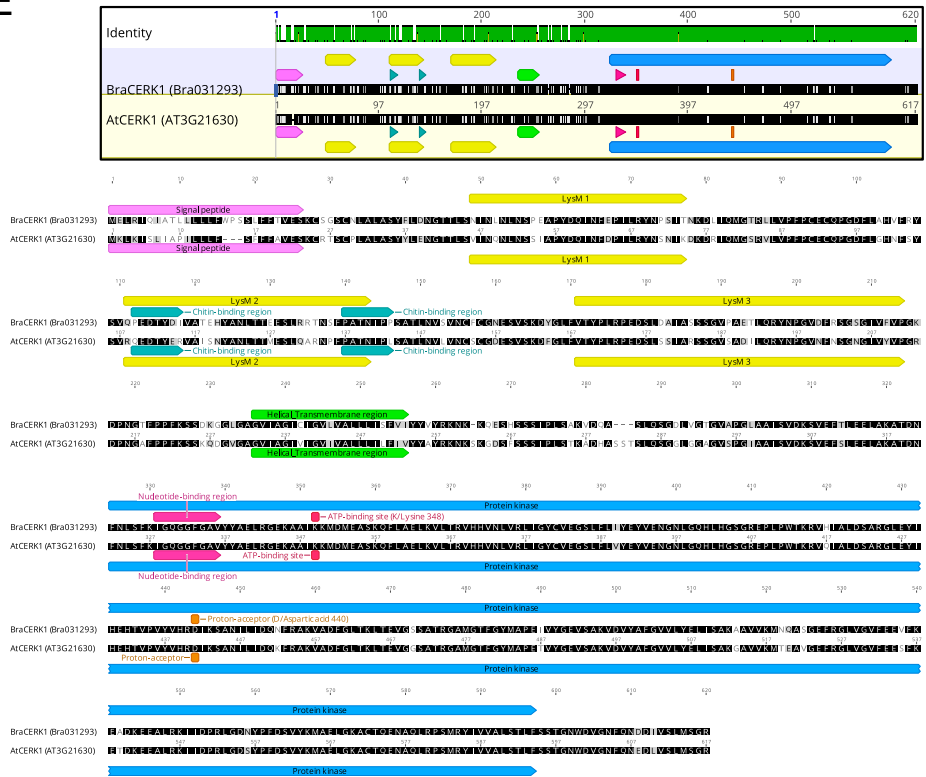
Figure 3 | Alignments and annotations of BraPRRs protein sequences

Alignments of 2 sequences: (A) BraFLS2 (Bra017563) and AtFLS2 (AT5G46330), (B) BraFLS2 (Bra022032) and AtFLS2 (AT5G46330), (C) BraEFR (Bra002305) and AtEFR (AT5G20480), (D) BraEFR (Bra006560) and AtEFR (AT5G20480), or (E) BraCERK1 (Bra031293) and AtCERK1 (AT3G21630) were generated and analyzed using Geneious 10.2.6. BraPRRs were manually annotated upon their reference protein AtPRR whose annotations are provided from UniProt (www.uniprot.org). All figures are extracted from Geneious 10.2.6.

Table 3 | Identity of functional domains and protein sequences between BraPRRs and AtPRRs

A

% Identical Sites (Align to AtFLS2)		
	BraFLS2	
Domain	Bra017563	Bra022032
SP	56.5 =	56.5
LRR1	91.3 =	91.3
LRR2	91.7 >	87.5
LRR3	79.2 >	66.7
LRR4	70.8 >	58.3
LRR5	70.8 >	62.5
LRR6	70.8 =	70.8
LRR7	75.0 >	62.5
LRR8	79.2 <	83.3
LRR9	83.3 >	66.7
LRR10	83.3 >	79.2
LRR11	83.3 =	83.3
LRR12	79.2 >	75.0
LRR13	87.5 >	83.3
LRR14	83.3 <	87.5
LRR15	73.9 =	73.9
LRR16	64.0 <	72.0
LRR17	82.6	100.0 (-)
LRR18	70.8	(-)
LRR19	66.7	62.5 (-)
LRR20	70.8 <	75.0
LRR21	87.5 >	66.7
LRR22	88.0 <	92.0
LRR23	72.0 =	72.0
LRR24	91.7 =	91.7
LRR25	83.3 =	83.3
LRR26	81.5 >	74.1
LRR27	100.0 >	76.0
LRR28	91.7 =	91.7
Total LRR	80.4 >	71.9
TM	66.7 <	73.7
Kinase domain	83.2 >	72.8
protein	80.0 >	72.2
Num. of higher identity	**15**	**6**

B

% Identical Sites (Align to AtEFR)		
	BraEFR	
Domain	Bra002305	Bra006560
SP	29.2 <	60.0
LRR1	78.3 >	69.6
LRR2	87.0 =	87.0
LRR3	78.3 <	82.6
LRR4	79.2 >	70.8
LRR5	82.6 >	78.3
LRR6	69.6 <	73.9
LRR7	87.0 >	82.6
LRR8	78.3 >	65.2
LRR9	77.3 <	86.4
LRR10	71.4 <	81.0
LRR11	83.3 <	95.8
LRR12	73.9 =	73.9
LRR13	82.6 =	82.6
LRR14	56.5 <	87.0
LRR15	73.9 =	73.9
LRR16	77.3 >	72.7
LRR17	82.6 >	73.9
LRR18	69.6 =	69.6
LRR19	82.6 =	82.6
LRR20	79.2 >	75.0
LRR21	84.6 >	76.9
Total LRR	77.8 <	78.2
TM	81.0 >	55.0
Kinase domain	81.1 <	83.2
Protein	76.7 <	78.2
Num. of higher identity	**10**	**10**

C

% Identical Sites (Align to AtCERK1)	
	BraCERK1
Domain	Bra031293
SP	50.0
LysM1	72.4
LysM2	63.6
LysM3	77.3
Total LysM	71.7
TM	76.2
Kinase domain	95.6
Protein	**83.5**

SP: Signal peptide
LRR: Leucine-rich repeat (LRR) domain
LysM: Lysin motif domain
TM: Transmembrane region
(-): Gap

Data extracted from Geneious 10.2.6

BraFLS2, BraEFR, and BraCERK1 were expressed in 1, 2, 4, 6-week-old Chinese cabbage leaves.

Followed by the comparative genomics between *B. rapa* cultivar line "Chiifu-401" and *A. thaliana* Col-0, the actual expression of *BraPRRs* in *B. rapa* hybrid cultivar line "Norang kimchi baechu" used for this study was required to examine. Furthermore, the data shown in **Table 2** presented the expression level of *BraPRR*s in the 7-week-old plant **(Tong et al., 2013)**, whereas the plant material in the first section of this study was collected in the 5 or 6-week-old Chinese cabbage. Hence, it was also necessary to investigate the expression level of *BraPRR*s in different stages of plants. Additionally, GUS accumulation driven by *AtFLS2* promoter could be observed in the 2-day-old seedling **(Beck et al., 2014)**, hypothesizing that *BraPRR*s are expressed in a very early stage during plant development. To examine the expression level change of *BraPRR*s during Chinese cabbage growth, the expression of *BraFLS2* (Bra017563), two *BraEFRs* (Bra002305 and Bra006560) and *BraCERK1* (Bra031293) was monitored by qRT-PCR in the 1-week-old cotyledon, and in the last elongated true leaves of 1, 2, 4 and 6-week-old plants.

As shown in the results **[Figure 4A]**, *BraFLS2* (Bra017563) and *BraCERK1* (Bra031293) were expressed in the 1-week-old cotyledon. In the true leaves of 1-week-old plant, *BraFLS2* (Bra017563) was downregulated to 0.19-fold and *BraCERK1* (Bra031293) was downregulated to 0.34-fold, comparable to the expression in the 1-week-old cotyledon. At 2 weeks, *BraFLS2* (Bra017563) was continuously downregulated but on the contrary, *BraCERK1* (Bra031293) was upregulated. In 4 weeks, both were upregulated. *BraFLS2* (Bra017563) was slightly upregulated, but *BraCERK1* (Bra031293) was strongly upregulated to 6.72-fold, comparable to the expression in the 1-week-old cotyledon. In 6 weeks, *BraFLS2*

(Bra017563) expression was reduced to the level of 2-week-old leaf. *BraCERK1* (Bra031293) expression was also reduced but at a slightly higher level, comparable to the level in the 1-week-old cotyledon. Expression of *BraFLS2* (Bra017563) kept at a quite low level unlike *BraCERK1* (Bra031293) during 6 weeks **[Figure 4A]**. Unfortunately, high similarity between two gene sequences of *BraEFR*s made the design of specific primers difficult. Furthermore, even with a pair of primers whose efficiency was 1.87, few valid value was gained by qPCR analysis, hypothesizing the expression level of *BraEFR*s might be too low to allow to detect by qPCR.

Therefore, the expression level of *BraEFR*s was examined by RT-PCR, using cleaved amplified polymorphic sequence (CAPS) analysis. PCR products were amplified with *EFR* CAPS primers **[Appendix A]**, binding a common region of *AtEFR* and *BraEFR*s. PCR products of *AtEFR*, *BraEFR1* (Bra006560) and *BraEFR2* (Bra002305) were in size of 656 nt, 659 nt and 644 nt, respectively. And *AtEFR* could be digested by *Pst*I/*Eco*RI into 152 nt, 342 nt and 162 nt fragments. *BraEFR1* (Bra006560) could be digested by *Eco*RI into 94 nt and 565 nt fragments. *BraEFR2* (Bra002305) could be recognized by neither *Pst*I nor *Eco*RI. As observed in **Figure 4B-a**, *BraEFR*s were expressed in all samples during 6 weeks, but with very low expression level compared to the level of *BraEF1α*. An approximately 300 nt fragment was also amplified from 1-week-old cotyledon, which have not been identified whether it was a random product or a gene related to *BraEFR* yet. Furthermore, a crude approximation of *BraEFR* expression **[Figure 4B-b]** was analyzed upon the intensity of bands **[Figure 4B-a]** by ImageJ. After normalization against *BraEF1α* expression level, *BraEFR*s were expressed 9.58×10^{-5}-fold in 1-week-old cotyledon and 4.49×10^{-5}-fold in 1-week-old true leaf. In 2 weeks, *BraEFR*s were upregulated to 5.60×10^{-5}-fold. And in 4 weeks, *BraEFR*s were continuously upregulated to 10.03×10^{-5}-fold. And unlike *BraFLS2* and *BraCERK1*,

in 6 weeks, *BraEFR*s were only slightly downregulated to 9.81×10^{-5}-fold and retained at a relatively high level as high as in 4 weeks.

In addition, previous studies were shown that *AtFLS2* expression could be induced by flg22 **(Smith et al., 2014)** and *AtEFR* expression could be also induced by flg22 **(Winter et al., 2007)**. To examine whether *BraEFR*s expression could be upregulated by elf18 elicitation, *EFR* CAPS was amplified using RT-PCR to detect the expression level of *BraEFR*s in Chinese cabbage leaves, which were treated by water and elf18 for 30 min. As shown in results, *BraEFRs* were induced at very low level compared to *BraEF1α*, and the unknown product with a size of 350 nt appeared in both treated samples **[Figure 4C-a]**. PCR products amplified in 35 cycles were digested by *Pst*I and *Eco*RI to differentiate *BraEFR1* (Bra006560) and *BraEFR2* (Bra002305). However, only the products with a size of approximate 650 nt were presented, suggesting that *BraEFR2* (Bra002305) was the main expressed gene between two *BraEFR*s, that was consistent with the previous data shown in **Table 2**. It might be difficult to detect *BraEFR1* (Bra006560) using restriction assay because of its extremely low expression level. Here, a crude approximation of *BraEFRs* expression change was also analyzed in the same way. *BraEFR*s in common was increased to 1.62-fold after elf18 treatment compared to the water-treated control **[Figure 4C-b]**.

Together, *BraFLS2* (Bra017563), *BraCERK1* (Bra031293) and *BraEFR*s were expressed more in 1-week-old cotyledon than in 1-week-old true leaf, then after keeping at a relatively low-level during 2 weeks, they were upregulated in 4 weeks in leaves of Chinese cabbage. *BraCERK1* (Bra031293) was generally expressed most among them, and *BraEFR*s were expressed at an extremely low-level. Between two *BraEFR*s, *BraEFR2* (Bra002305) was mainly expressed and upregulated after elf18 elicitation.

A

B

a

b

C

a

b
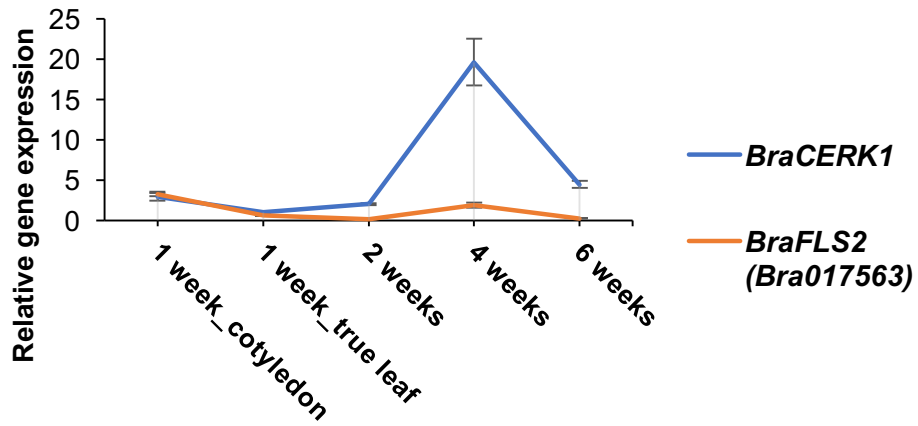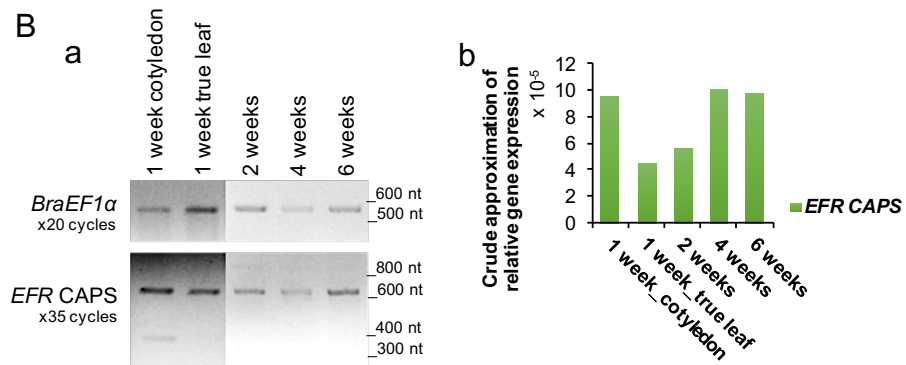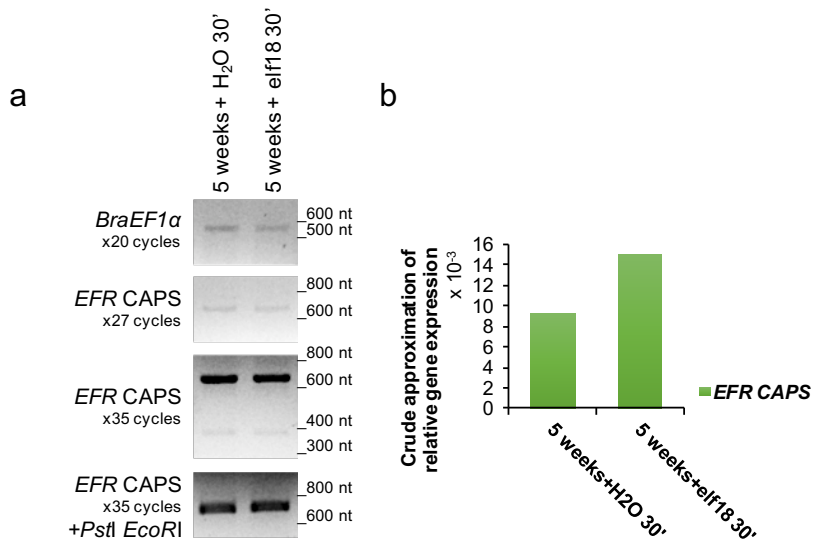
Figure 4 | Expression of *BraPRR* candidates in Chinese cabbage leaf

Leaf discs were collected from 1-, 2-, 4- and 6-week-old Chinese cabbage without any treatment before RNA extraction. 5-week-old Chinese cabbage leaf discs challenged with water (H_2O) and elf18 in 30 minutes **(Figure 1)** were selected as template in this assay. **(A)** *BraCERK1* and *BraFLS2* (Bra017563) gene expression was monitored by qRT-PCR. Expression levels were normalized against housekeeping gene *BraEF1α* gene expression in three technical replicates ± standard error. **(B)** and **(C)** *BraEF1α* and *EFR* CAPS were amplified and resolved on 1.5% (*BraEF1α*) and 2% (*EFR* CAPS) agarose. RT-PCR product of *EFR* CAPS was digested by enzymes *Pst*I and *Eco*RI for 1 hour then resolved on 2% agarose. Histograms in **(b)** were generated by ImageJ aiming to present relative gene expression level of *EFR* CAPS in **(a)** normalized against *BraEF1α* gene expression. The value was calculated according to formula:

Crude approximation of relative gene expression=$\dfrac{\frac{gene_{ImageJ}}{2^{cycles}}/5\ \mu L}{\frac{BraEF1\alpha_{ImageJ}}{2^{20}}/10\ \mu L}$.

Cloning and expression library of PRRs were created using Golden Gate Assembly.

Since the gene expression was revealed in *B. rapa* cultivar "Norang kimchi baechu", *BraFLS2* (Bra017563), *BraEFR1* (Bra006560), *BraEFR2* (Bra002305) and *BraCERK1* (Bra031293) were cloned from genomic DNA (gDNA) in order to create the expression library for revealing gene function in further study. From here on, Bra017563 is called as *BraFLS2*. Bra006560 which is more similar to *AtEFR* is called as *BraEFR1*. Bra002305, the one which was mainly expressed between two *BraEFR* candidates is called as *BraEFR2*. And Bra031293 is called as *BraCERK1*.

To take our gene length (approximately three to four Kb) into account, Golden Gate Assembly technology was chosen to clone *PRR* genes and construct expression library **[Figure 5]**. Each gene of *BraPRR*s and *AtPRR*s was divided into three to four of approximately 1 kb modules to create the modules library, which was carried by *E. coli* strain DH5α [**Appendix B**]. After annotating and comparing the sequencing results of the cloned genes from "Norang kimchi baechu" to the reference genes from "Chiifu-401", two *BraFLS2* genes were 100% matched in module 1, 2 and 4 sequences. In module 3, the identity of two genes was 100% in exons, but they were a few differences in intron, a 6 bp sequence AGGGCC was inserted at the site corresponding to the 3,298 location of reference "Chiifu-401" gene. And 3 nucleotides were mismatched in a T-rich region from location 3,318 to 3,331, TTTTTTTTTTT-T in Norang kimchi baechu compared to TCTTTATTTTTCT in Chiifu-401. However, these were possibly due to the difficulty of sequencing in a T-rich region. For *BraCERK1*, modules 2 and 3 were 100% identical. Only 1 nucleotide in exon of module 1 was mutated (T24 in Chiifu-401 was replaced by G24 in Norang kimchi baechu), but it was a synonymous mutation. For *BraEFR*s, the cloning of *BraEFR1* from gDNA of Norang kimchi baechu was failed, so we synthesized this

43

gene.

All modules were assembled into backbone vector and fused with C-terminal 6xHA or YFP tag to construct the expression library **[Appendix B]**. All constructs were under the control of 35S promoter. We also created the expression vectors of *AtCERK1* and *BraCERK1*, fused with C-terminal 6xHA or YFP tag, under the control of *CERK1* native promoters containing ~ 1kb upstream of start codon.

To reveal whether BraPRR-mediated responses require kinase activity, kinase dead versions of *BraFLS2*, *BraEFR2* and *BraCERK1* **[Appendix B]** were generated using site-directed mutagenesis. The proton acceptor residue, aspartic acid of BraFLS2 (D999) or BraEFR2 (D846), was point-mutated and replaced by asparagine (N) **[Figure 3A and 3C]**. For BraCERK1, we point-mutated the lysine residue (K349) into asparagine (N) instead of the ATP-binding site K348 by confounding with the ATP-binding site of *AtCERK1* (K349) **[Figure 3E]**. K349 of BraCERK1 is directly located next the ATP-binding site of kinase (K348), and belong to ATP-binding region (327-IGQGGFGAVYYAELRGEKAAIKK*-349), so even with an unexpected mutated site K349 (the expected one was K348), this kinase dead version of BraCERK1 was still used in following study.

All expression vectors of *AtPRR*s, *BraPRR*s and the kinase dead version of *BraPRR*s were transformed to *A. tumefaciens* strain AGL1 **[Appendix B]**.

Primer design

*Bsa*I sequence

Mod F/R

Overhang

Modules cloning

mod1F   mod2F   mod3F

DNA template

mod1R   mod2R   mod3R

Purified PCR products

mod1

mod3

mod2

pUC19B   →   *Sma*I   +   Ligation

mod1   mod2   mod3

Assembly

Tag

pICH41155   →   +   *Bsa*I digestion

pICH86988   →   +

mod3   Tag

mod1   mod2

pICH86988

Ligation

mod1   mod2

mod3

Tag

Final construction

pICH86988
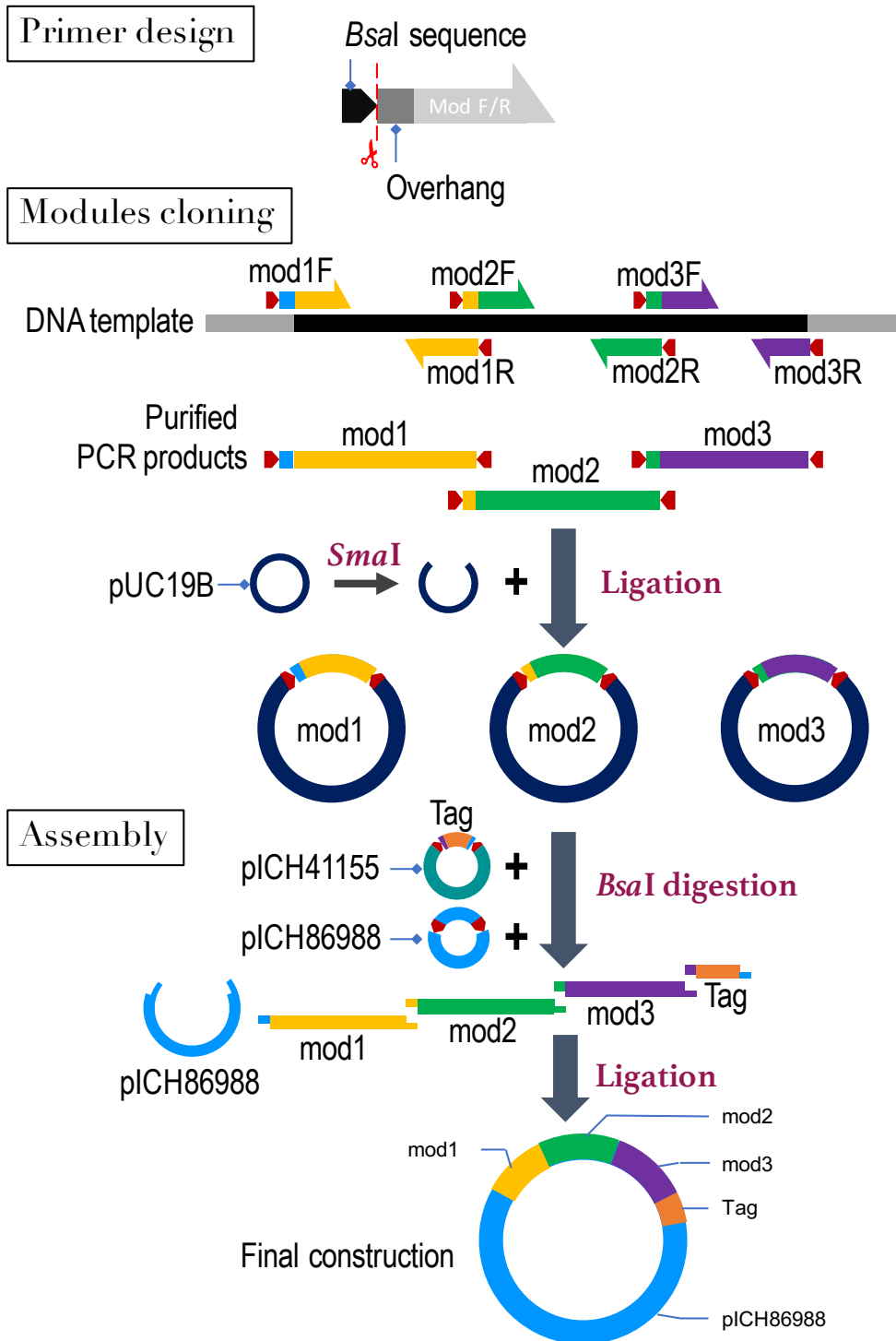
Figure 5 | Cloning scheme for the construction of *PRR*-library by Golden Gate Assembly

In the first step, primer design, all primers are designed to add a 4 nucleotide overhang specific to bilateral DNA fragments in the final construct, and a *Bsa*I recognition site subsequently added at the end. In the second step, modules cloning, modules are amplified by RT-PCR, and are ligated into pUC19B cloning vector by *Sma*I/T4 ligase. The cloning constructs are confirmed by *Bsa*I-digestion and by sequencing. In the third step, assembly, the confirmed module-cloning constructs, backbone vector pICH86988 and vector carrying 6xHA or YFP-tag are ligated and assembled simultaneously to the final construction by *Bsa*I/T4 ligase.

mod F/R: the forward or reverse primer

mod#: module#

mod#F: the forward primer of module#

mod#R: the reverse primer of module#

✂: *Bsa*I recognition site

Functional analysis of *BraFLS2*, *BraEFR1*, *BraEFR2* and *BraCERK1* by transient expression in *N. benthamiana*

BraPRR-YFPs were localized at the plasma membrane of plant cells.

In plant, PRRs are known so far as cell surface localized protein. To reveal whether *BraPRR*s in this study were plasma membrane (PM) localized proteins, the subcellular localizations of *BraFLS2-YFP*, *BraEFR1-YFP*, *BraEFR2-YFP*, *BraCERK1-YFP, AtFLS2-YFP* and *GFP* were analyzed in the leaves of *N. benthamiana*. GFP is well known as a fluorescent protein localized in the cytoplasm and nucleus, and AtFLS2 is one of the well-characterized PRRs which is demonstrated that it is localized at PM of cells in most tissues of plant **(Robatzek et al., 2006)**. Confocal microscopy, as shown in **Figure 6A**, revealed that all BraPRRs were accumulated at the epidermal cells and guard cells. And BraPRRs were obviously localized at the cell periphery as well as control AtFLS2 and GFP **[Figure 6A, +H$_2$O]**. In the plasmolyzed leaf tissues resulted from 1 M NaCl, Hechtian strands, a characteristic of direct physical connection between PM and cell wall, were observed in the cells expressing BraFLS2, BraEFR1 and BraEFR2 as well as positive control AtFLS2. However, plasmolysis in the cells expressing GFP did not result in Hechtian strands **[Figure 6A, +1M NaCl]**. These results indicated that BraFLS2, BraEFR1 and BraEFR2 were obviously localized at the PM.

Furthermore, the fluorescence intensities of BraEFR1 and BraEFR2 were weaker than BraFLS2, indicating a lower transient expression level than BraFLS2. And overexpressed BraEFR1 and BraEFR2 were also accumulated in the endoplasmic reticulum (ER), indicating a protein folding process of BraEFRs.

Interestingly, the plant cells overexpressing BraEFRs showed a lower salt tolerance than BraFLS2. Treated with 1 M NaCl, plasmolysis in the cells overexpressing BraFLS2 can be continued within approximately 30 min until the cell was dehydrated to a small, round and alive protoplast **[Figure 6A, +1M NaCl]**. However, the fluorescent signal of the cells overexpressing BraEFRs suddenly disappeared when plasmolysis progressed to a certain extent within approximately 15 min after 1 M NaCl treatment. The vanishing of the fluorescent signal was probably due to the cell death under salt stress.

Besides, the expression vector of *BraCERK1-YFP* was driven by its native promoter (pCERK1), which differed from 35S promoter of *BraFLS2* and *BraEFR*s in this subcellular localization analysis, because overexpression BraCERK1 in *N. benthamiana* induced cell death [**Figure 8**]. Unfortunately, the expression of pBraCERK1 : BraCERK1-YFP induced the cell death too **[Figure 8]**, leading to trouble with observing BraCERK1 expression and plasmolysis in leaf tissue under confocal microscopy. Although failed to observe plasmolysis and Hechtian strands displayed in the cells of *N. benthamiana*, BraCERK1 was supposed to be localized at the PM as well as BraFLS2 and BraEFRs.

B +100 nM flg22

GFP/YFP | Merged | GFP/YFP[a]

GFP

AtFLS2

BraFLS2

50
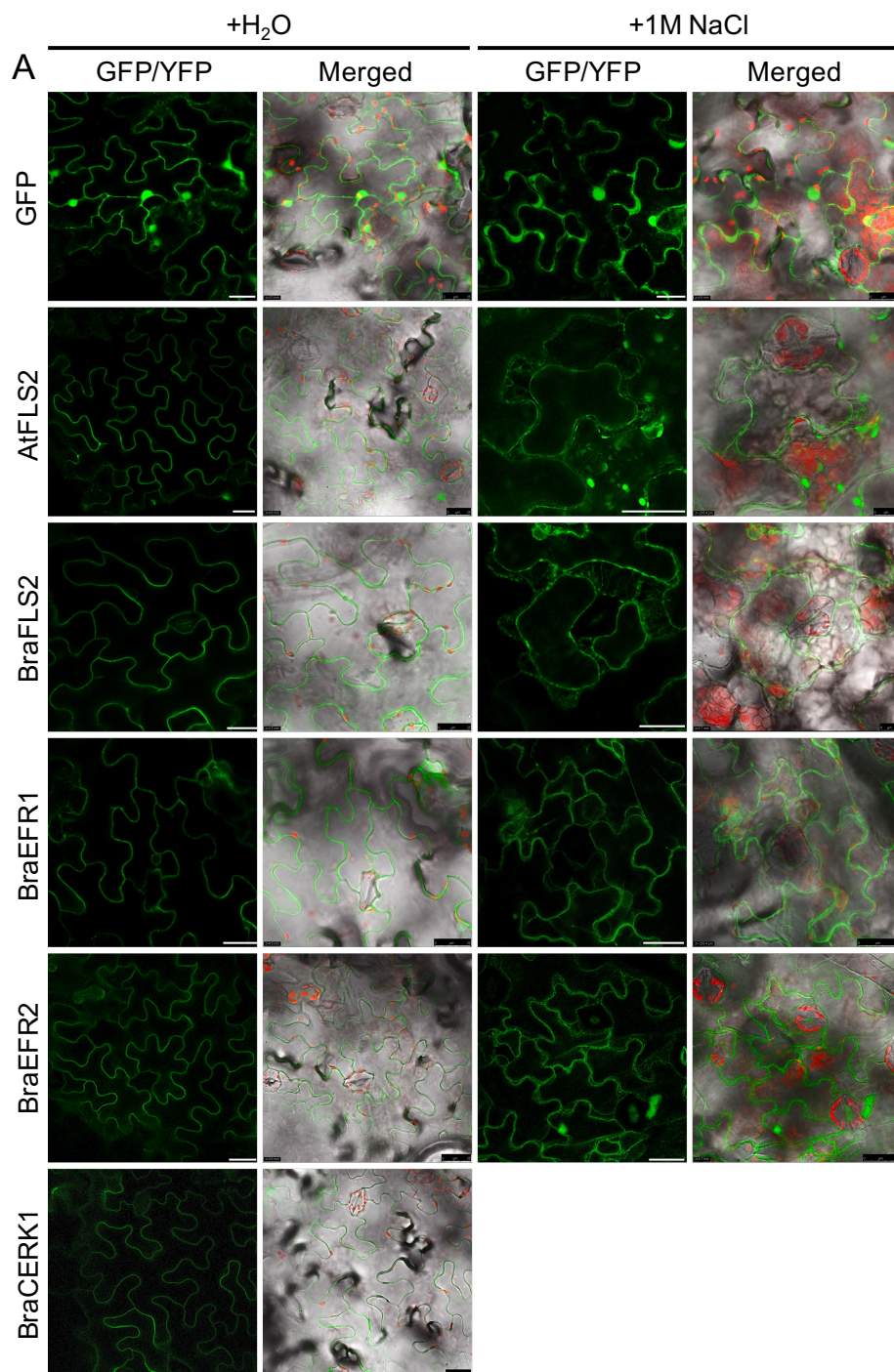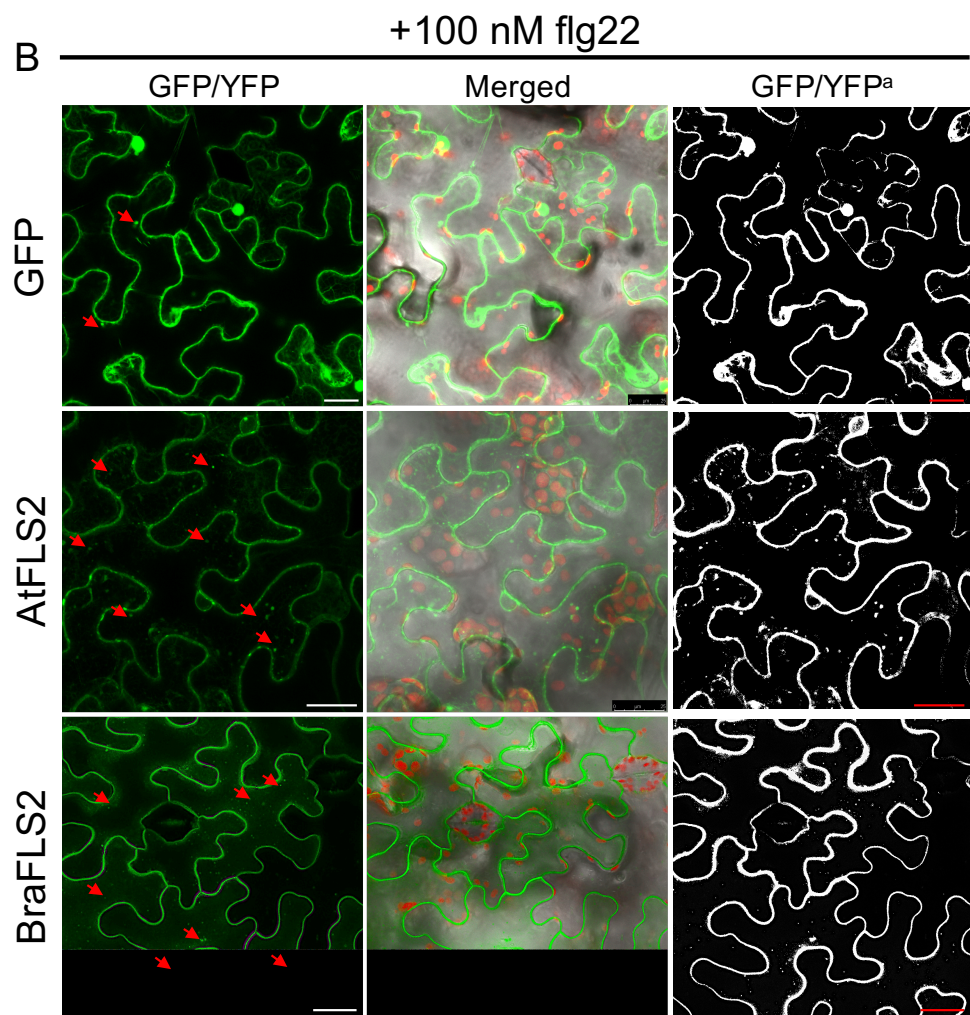
Figure 6 | Localization of BraPRRs and endocytosis upon flg22 perception in *N. benthamiana*

Confocal micrographs record the leaf epidermal cells of 6-week-old *N. benthamiana* transiently expressing *GFP*, *AtFLS2*, *BraFLS2*, *BraEFR1*, *BraEFR2* or *BraCERK1* fused with *YFP* tag using *Agrobacterium*-mediated infiltration. Expression of *GFP*, *AtFLS2*, *BraFLS2*, *BraEFR1*, and *BraEFR2* were under the control of 35S promoter and expression of *BraCERK1* was under the control of native promoter. Two days post-infiltration, leaf discs were collected and challenged with (A) water H_2O or 1 M NaCl for 15 to 45 min and with (B) 100 nM flg22 for 10 to 30 min before imaging. (B) Red arrows indicate the endocytic vesicles. Images of GFP/YFP[a] were generated from the GFP/YFP images on the left into black and white by using ImageJ. Chloroplast auto-fluorescence shown in the merged images was recorded in red. Fluorescence intensity is variable for each image and is not representative of the expression level. (Scale bar: 25 μm.)

BraFLS2 endocytosis was induced upon flg22 perception.

Previous study has shown that AtFLS2 is rapidly internalized into endocytic vesicles after flg22 treatment **(Robatzek et al., 2006)**. To reveal whether BraFLS2 internalization can be induced upon flg22 treatment, the leaf epidermal cells of *N. benthamiana* overexpressing *BraFLS2-YFP*, *AtFLS2-YFP* or *GFP* were challenged with 100 nM flg22 and observed under confocal microscopy **[Figure 6]**. Obviously, a large number of BraFLS2 endocytic vesicles were induced within 10 min after flg22 treatment, as well as AtFLS2. In contrast, the GFP endocytic vesicles were rarely observed after flg22 treatment. These results indicated that BraFLS2 recognized flg22 and its internalization could be induced by flg22.

BraEFR2 expression induced elf18-triggered ROS production.

EFR gene has been found so far confined to the *Brassicaceae* family **(Kunze et al., 2004; Zipfel et al., 2006)**, *N. benthamiana* as a specie from *Solanaceae* family could not perceive elf18 and trigger PTI responses. However, *N. benthamiana* expressing AtEFR gains elf18 responsiveness **(Lacombe et al., 2010)**. To reveal whether expression of *BraEFRs* in *N. benthamiana* conferred gain of elf18 responsiveness and triggered PTI responses, oxidative burst in *N. benthamiana* expressing *GFP*, *AtEFR*, *BraEFR1*, *BraEFR2* and the kinase dead version of *BraEFR2* (*BraEFR2_D846N*) was detected in response to elf18. As shown in results **[Figure 7]**, upon 50 nM elf18 treatment, only *BraEFR2* and positive control *AtEFR* overexpressing lines induced ROS production, and both total ROS production were significantly accumulated, comparable to negative control *GFP* overexpressing line. No ROS accumulation could be observed in *GFP*, *BraEFR1* and *BraEFR2_D846N* overexpressing lines. Taken together, these results indicated that *BraEFR2* expression conferred gain of elf18 perception and triggered ROS response, and that required BraEFR2 kinase activity, but BraEFR1 probably could not function to trigger ROS burst. In addition, *Agrobacterium*-mediated transient expression of *BraEFR*s in *N. benthamiana* did not affect ROS production in response to flg22, indicating that the plant immune system of *N. benthamiana* expressing *BraEFR*s functioned normally.

+ 50 nM elf18
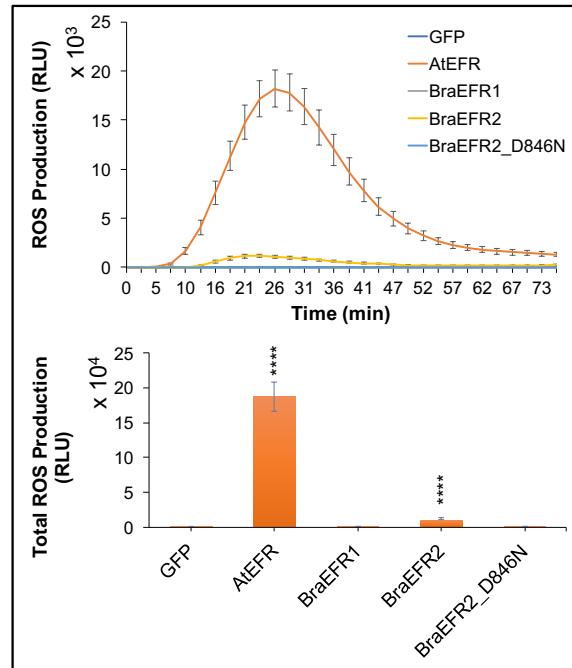
+ 50 nM flg22
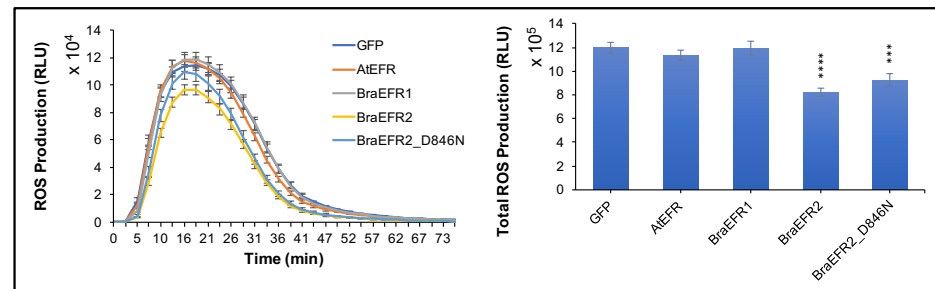
+ H$_2$O
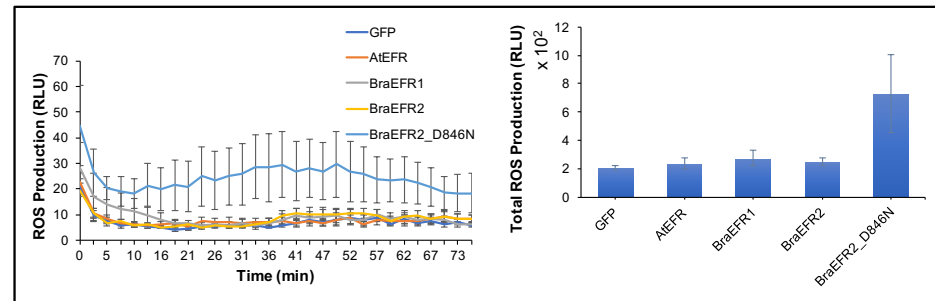
Figure 7 | elf18-induced ROS production in *N. benthamiana* transiently expressing *BraEFR1* and *BraEFR2*

6-week-old *N. benthamiana* leaves transiently over-expressing *GFP*, *AtEFR*, *BraEFR1*, *BraEFR2* and *BraEFR2-D846N* fused with *6xHA* tag using *Agrobacterium*-mediated infiltration. One day post-infiltration, leaf discs were collected and kept on water in a 96-well plate overnight. Two days post-infiltration, leaf discs were challenged with 50 nM elf18, 50 nM flg22 or H_2O before measurement. For each condition, 16 leaf discs were collected. ROS production (Relative Light Unit) was measured by chemiluminescence of oxidized luminol. Kinetic and total ROS production were measured for 75 minutes in three biological replicates ± standard error. Asterisks indicate significant differences compared to GFP samples by Student's T-test. ****: $p < 0.0001$ ***: $0.0001 < p < 0.001$ **: $0.001 < p < 0.01$ *: $0.01 < p < 0.05$ ns: $p \geq 0.05$.

BraCERK1 expression led to chitin-independent cell death.

The transient expression of *AtCERK1* induced pathogen-independent cell death that required its kinase activity **(Pietraszewska-Bogiel, 2013)**. To investigate whether *BraCERK1* expression could induce chitin-independent cell death, *GFP*, *AtCERK1-6xHA*, *BraCERK1-6xHA* and *BraCERK1_K349N-6xHA* driven by 35S promoter were transiently expressed in *N. benthamiana* leaves with a series of inoculum density (OD_{600}). Moreover, the transient expression of *BraCERK1-YFP* driven by *BraCERK1* native promoter was examined, that was mentioned in subcellular localization analysis **[Figure 8]**. Overexpression of *BraCERK1* induced cell death within 0.7-day post infiltration (dpi) at high inoculum density (OD_{600}=0.5) and induced cell death within 1 dpi at middle inoculum density (OD_{600}=0.05), as consistent as *AtCERK1*. However, overexpression of *BraCERK1* induced cell death within 2 dpi at low inoculum density (OD_{600}=0.005), later than *AtCERK1*. Overexpression of *BraCERK1_K349N* only induced cell death at high inoculum density (OD_{600}=0.5) within 0.7 dpi, as soon as *BraCERK1* and *AtCERK1*, however, decreasing the inoculum density to OD_{600}=0.05, it could not induce cell death, indicating that kinase activity affected *BraCERK1*-mediated cell death. Transient expression of *BraCERK1-YFP* driven by *BraCERK1* native promoter induced cell death within 1 dpi at high inoculum density (OD_{600}=0.4) but as well as *BraCERK1_K349N* could not induce cell death at middle and low inoculum density (OD_{600}=0.04 to 0.004). Taken together, transient expression of *BraCERK1* in *N. benthamiana* leaves induced cell death that affected by the activity of kinase and promoter.

In this section, all expression constructs were confirmed to function expectedly, allowing to use them for functional complementation assays in stable transgenic lines.

57
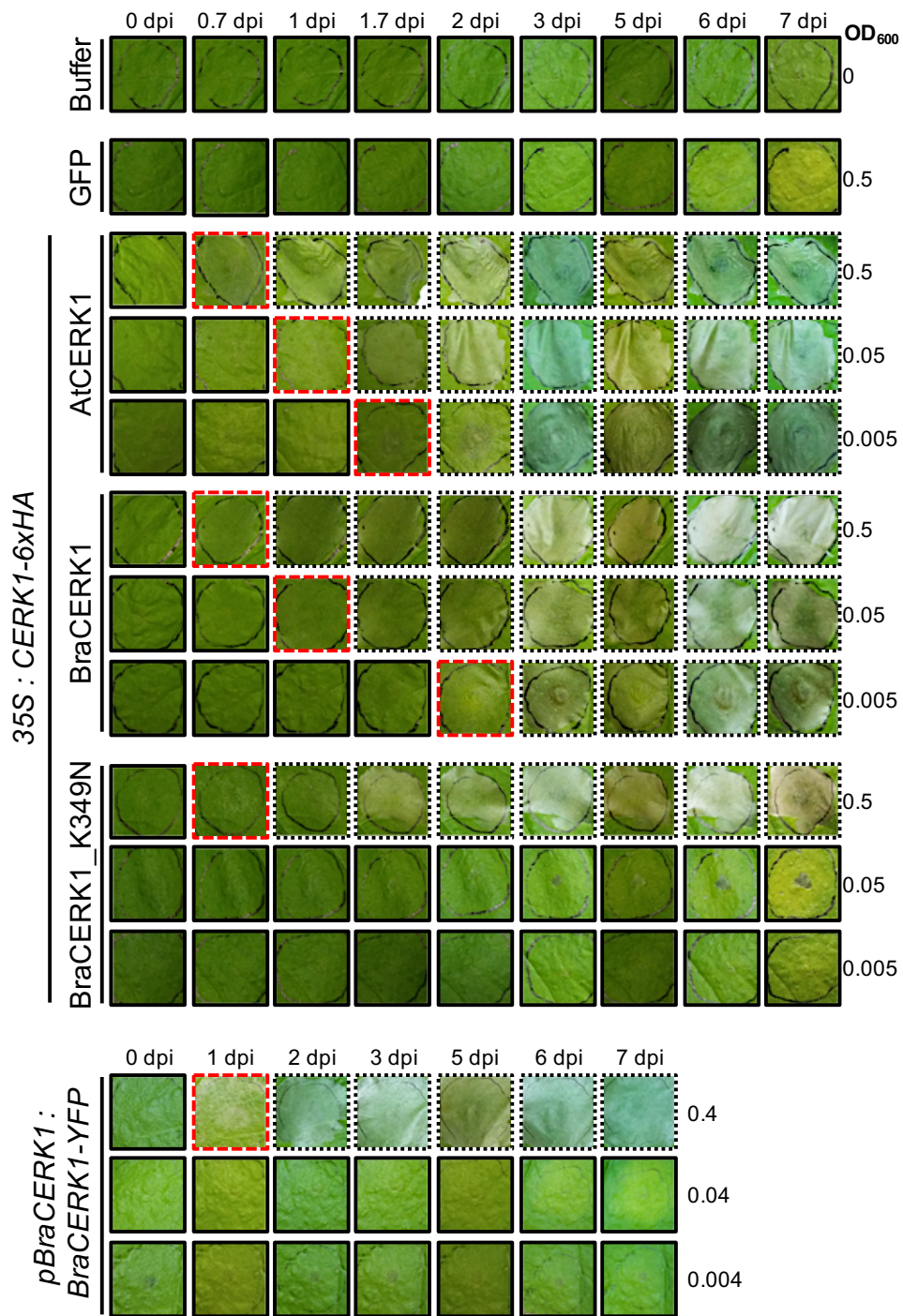
Figure 8 | Cell death induced by BraCERK1 in *N. benthamiana*

6-week-old *N. benthamiana* leaves transiently over-expressing *GFP*, *AtCERK1*, *BraCERK1* and *BraCERK1_K349N* fused with *6xHA* tag or *BraCERK1* fused with *YFP* tag under the control of *BraCERK1* native promoter using *Agrobacterium*-mediated infiltration. The concentration of *A. tumefaciens* (OD_{600}) and the time points were indicated. dpi indicated day(s) post infiltration. Dotted box indicated the appearance of cell death and the red dotted box indicated the first observation of cell death.

Functional complementation in *Arabidopsis* transgenic *BraPRR*-expressing lines

Screening of Arabidopsis transgenic PRR expressing lines

To investigate whether the expression of BraPRR protein could complement the defect of PAMP perception in the *Arabidopsis prr* mutant, *Arabidopsis* transgenic *AtPRR* expressing lines, *BraPRR* expressing lines and the kinase dead version of *BraPRR* expressing lines were generated and screened by kanamycin resistance to produce homozygous lines **[Appendix C]**. All transgenes were fused with C-terminal 6xHA tag. For *FLS2* transgenic lines, the expression of transgenes was driven by *CaMV* 35S promoter, and performed on two different background plants, *fls2 efr cerk1* (*fec*) triple mutant or *fls2* single mutant to reveal the effect from background plant. The expression of transgenes in *EFR* transgenic lines was driven by *CaMV* 35S promoter and performed only on one background plant *fec* mutant. For *CERK1* transgenic lines, expression of transgenes was driven by both *CaMV* 35S promoter and *CERK1* native promoter and performed on *fec* mutant.

After two generations, the segregation of kanamycin-resistant plant versus susceptible plant (R:S) of T2 lines demonstrated that most transgenic lines only have single copy of the transgene in the genomic DNA, because the ratio of R:S approached 3:1 **[Appendix C]**. The screening of homozygous lines is still in progress.

The growth phenotype of these transgenic plants was shown that T3 homozygous plants of transgenic *EFR* expressing lines grew nearly as well as wild type Col-0 and background *fec*. Conversely, some of T2 plants in transgenic *FLS2* and *CERK1* expressing lines grew smaller than Col-0 and background plant in the

soil. For example, *AtFLS2* transgenic lines F4-2 and F4-5, *BraFLS2* transgenic line F5-1, *BraFLS2_D999N* transgenic line F6-3 and F6-6 grew smaller than Col-0 and *fls2*. In addition, some plants of *BraFLS2* transgenic line F5-4 grew not only smaller than other lines, but also had different leaf phenotype: the first 5 to 6 leaves were round and dark green then became yellow, and from the 7th leaf, the leaves became curled up and crinkled. In *CERK1* transgenic lines, all *BraCERK1* and *BraCERK1_K349N* transgenic lines grew slightly smaller than Col-0 and *fec*, but *BraCERK1* transgenic line C2-2 and *BraCERK1_K349N* transgenic line C3-5 were obviously small. After all, T2 plants still segregated and be unstable in phenotype, the growth phenotype assay is required to reveal again with T3 homozygous plants in a sterile environment.

T2 transgenic *FLS2* and *CERK1* overexpressing lines and T3 homozygous transgenic *EFR* overexpressing lines were tested in following functional complementation assays.

BraFLS2 and BraEFR2 expression complemented flg22 and elf18-triggered seedling growth inhibition in fls2 and fec mutants.

In previous study, long exposure for 2 weeks to 100 nM flg22 could strongly inhibit the growth of *Arabidopsis* Col-0 seedling to half-maximal growth reduction, and the effect was dose-dependent **(Gómez-Gómez et al., 1999).** To determine whether the expression of *BraPRR*s conferred gain of PAMP perception, PAMP-triggered seedling growth inhibition (SGI) assay was performed on *FLS2* and *EFR* transgenic lines **[Figure 9]**.

In response to flg22 **[Figure 9A]**, a significant dose-dependent inhibition of seedling growth was observed in wild type Col-0 seedling, consistent with the results shown in previous study **(Gómez-Gómez et al., 1999)**. In contrast, the background plants neither *fls2* mutant nor *fec* mutant was sensitive to flg22 treatment, consistent with the results shown in previous study **(Zipfel et al., 2006; Häweker et al., 2010)**. Interestingly, the seedlings of almost all transgenic *FLS2* expressing T2 lines were sensitive to flg22 along with the dose increase. Seedling growth of *BraFLS2* transgenic lines F5-2, F5-4 and F5-7, as well as *AtFLS2* transgenic lines F1-1 and F1-2 was strongly inhibited upon flg22 treatment. *BraFLS2_D999N* transgenic lines F6-3, F6-5 and F6-6 in the background of *fls2* mutant, as well as F3-1, F3-2 and F3-4 in *fec* mutant, obviously reduced the sensitivity to flg22 compared to *BraFLS2* transgenic lines. Interestingly, the reduction of sensitivity to flg22 was less in the background of *fls2* mutant than in the *fec* mutant. In the background of *fls2* mutant, *BraFLS2* transgenic lines F5-1, F5-2, F5-4 and F5-7 were more sensitive to 100 nM and 1000 nM flg22 treatments in SGI assay than *AtFLS2* transgenic lines F4-1, F4-2 and F4-5. Conversely, in the *fec* mutant background, *BraFLS2* transgenic line F2-1 was less sensitive than *AtFLS2* transgenic lines F1-1 and F1-2 to 1000 nM flg22

treatment. Compared *BraFLS2_D999N* transgenic lines in the background of *fls2* to those in the *fec* mutant background, transgenic seedlings in the *fec* mutant background (F3-1, F3-2 and F3-4) seemed to be slightly more sensitive to high dose flg22 than those in the *fls2* mutant background (F6-3, F6-5 and F6-6). Together, the expression of *BraFLS2* conferred gain of flg22 responsiveness and complemented flg22-triggered seedling growth inhibition in *Arabidopsis fls2* and *fec* mutants. *BraFLS2*-mediated seedling growth inhibition partially required its kinase activity. It seemed to have another mechanism to replace the role of kinase and guarantee the process of seedling growth inhibition after flg22 perception.

In response to elf18 **[Figure 9B]**, consistently with flg22 treatment, seedling growth of wild type Col-0 was significantly and gradually inhibited along with elf18 dose increase, and the plants of background plant *fec* mutant were insensitive to elf18 dose change **(Gómez-Gómez et al., 1999; Zipfel et al., 2006)**. However, the positive control T3 homozygous *AtEFR* transgenic line E1-1-2 was insensitive to elf18 treatment. Two *BraEFR1* transgenic lines E2-4-2 and E2-5-5 were also insensitive to elf18 treatment. Conversely, *BraEFR2* transgenic lines E4-1-5 and E4-4-1 were shown a strong seedling growth inhibition upon elf18 treatment and more sensitive to elf18 dose change than Col-0. *BraEFR2_D846N* transgenic lines E5-1-1 were less sensitive to elf18 treatment than *BraEFR2* transgenic lines. However, unlike *BraFLS2_D999N* transgenic lines which were slightly inhibited by flg22, E5-1-1 was strongly inhibited as Col-0. Although failed to compare with *AtEFR* transgenic lines, the results demonstrated that the expression of *BraEFR2* in *fec* mutant complemented elf18 responsiveness, and *BraEFR2* kinase activity affected but only with a limited role for the regulation of seedling growth inhibition. *BraEFR1* might not function, consistently with the observation in oxidative assay performed using *N. benthamiana* leaves **[Figure 7]**.

A
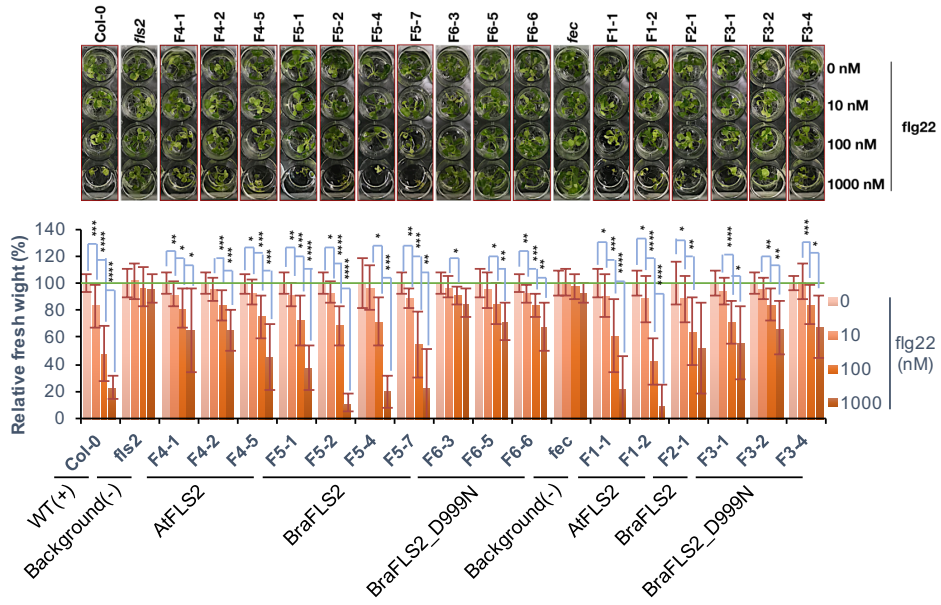
B
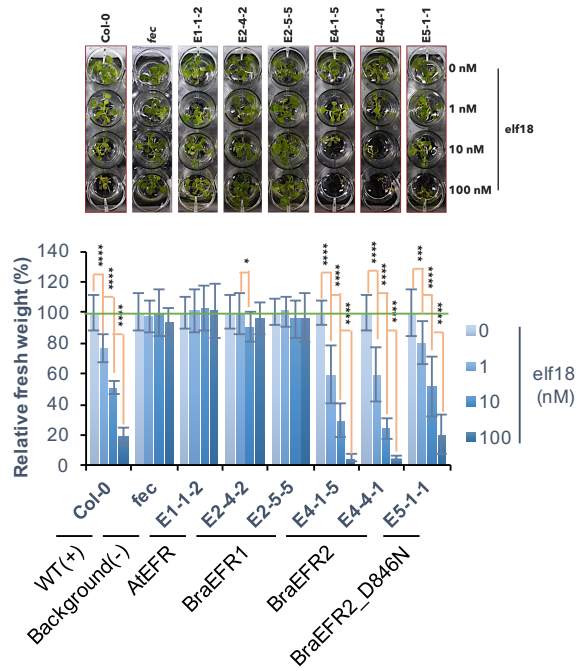
Figure 9 | Seedling growth inhibition in transgenic *FLS2* and *EFR* expressing lines

4-day-old seedlings of Col-0, *fec*, *fls2*, transgenic *FLS2* and *EFR* over-expressing lines were challenged with H_2O, flg22 (10 nM, 100 nM and 1000 nM) or elf18 (1 nM, 10 nM and 100 nM) in MS liquid medium for an additional 10 days under LD condition. For each condition, 12 seedlings (2 per well) were collected. Fresh seedling weight was measured using high precision digital balance. Mean of the fresh weight of samples with H_2O-treatment was assigned the value 100%. Values are presented as mean of relative fresh weight in three biological replicates ± standard error (Exception: only two biological replicates in F5-7 line, and only one biological replicate with 6 seedlings per condition in F5-4 line). Red box indicates the visible seedling growth inhibition on gross inspection. Asterisks indicate significant differences between each concentration compared by Student's T-test. ****: $p < 0.0001$ ***: $0.0001 < p < 0.001$ **: $0.001 < p < 0.01$ *: $0.01 < p < 0.05$ ns: $p \geq 0.05$.

Expression of BraPRRs led to PAMP responsive ROS production in fls2 or
fec mutant.

To further confirm the functional complementation of BraPRRs in defense responses of *fls2* or *fec* mutant, the oxidative burst assay was performed on transgenic *FLS2*, *EFR* and *CERK1* overexpressing lines **[Figure 10]**.

Upon 50 nM flg22 elicitation, wild type Col-0 induced ROS production within 1 min but the background line *fls2* mutant could not **[Figure 10A]**. *BraFLS2* transgenic line F5-2 induced ROS production within 1 min as fast as Col-0, and with a total ROS accumulation significantly higher than the background line *fls2* mutant. Two other *BraFLS2* transgenic lines F5-1 and F5-4 also induced ROS production, with a total production that is extremely slight but significantly different to the background line *fls2* mutant. The positive control *AtFLS2* transgenic line F4-5 induced an extremely slight ROS production. Although the total ROS accumulation of F4-5 was significant compared to *fls2* mutant, the ROS response was far from the strength of Col-0. *BraFLS2_D999N* transgenic lines F6-3 and F6-6 behaved as the background line *fls2* mutant **[Figure 10A]**. Although the overexpression of *BraFLS2* did not induce a strong ROS production as expected, it still complemented flg22 responsiveness in *fls2* mutant. In addition, BraFLS2-mediated ROS production required kinase activity.

Upon 50 nM elf18 elicitation, elf18-triggered ROS production was complemented in *BraEFR2* transgenic T3 homozygous lines E4-1-5 and E4-4-1, and ROS response was nearly as strong as Col-0, but its induction was delayed approximately 3 min **[Figure 10B]**. Unlike *BraFLS2_D999N* transgenic lines, the kinase dead version of *BraEFR2*, *BraEFR2_D846N* E5-1-1, induced a very slight but significant ROS accumulation, comparable to the background line *fec* mutant. Consistent with SGI analysis, neither *AtEFR* transgenic line E1-1-2 nor *BraEFR1*

transgenic lines E2-4-2 and E2-5-5 induced a significant ROS production, as well as the *fec* mutant **[Figure 10B]**. These results suggested that BraEFR2 expression conferred gain of elf18 perception, and the kinase activity of BraEFR2 significantly affects ROS production in the *fec* mutant.

Upon 500 µg/mL chitin elicitation, Col-0 was shown a normal ROS production, however *AtCERK1* transgenic line C1-1, *BraCERK1* transgenic line C2-2 and *BraCERK1_K349N* transgenic lines C3-2 and C3-5 were shown an abnormal ROS production which was accumulated constantly even after 114 min **[Figure 10C]**. Unlike the strong ROS response generated in *AtCERK1* transgenic line C1-1, the ROS responses were induced slighter and less in *BraCERK1* transgenic line C2-2 and *BraCERK1_K349N* transgenic lines C3-2 and C3-5 than in Col-0. *BraCERK1_K349N* transgenic lines C3-2 and C3-5 produced total ROS accumulation that were similar with *BraCERK1* transgenic line C2-2, but their ROS inductions were delayed approximately 20 min compared to *BraCERK1* transgenic line C2-2. No ROS accumulation was observed in the background line *fec* mutant and two *BraCERK1* transgenic lines C2-3 and C2-4. To sum up, *BraCERK1* complemented chitin perception via its overexpression in *fec* mutant and mediated ROS burst in a limited kinase-dependent manner.
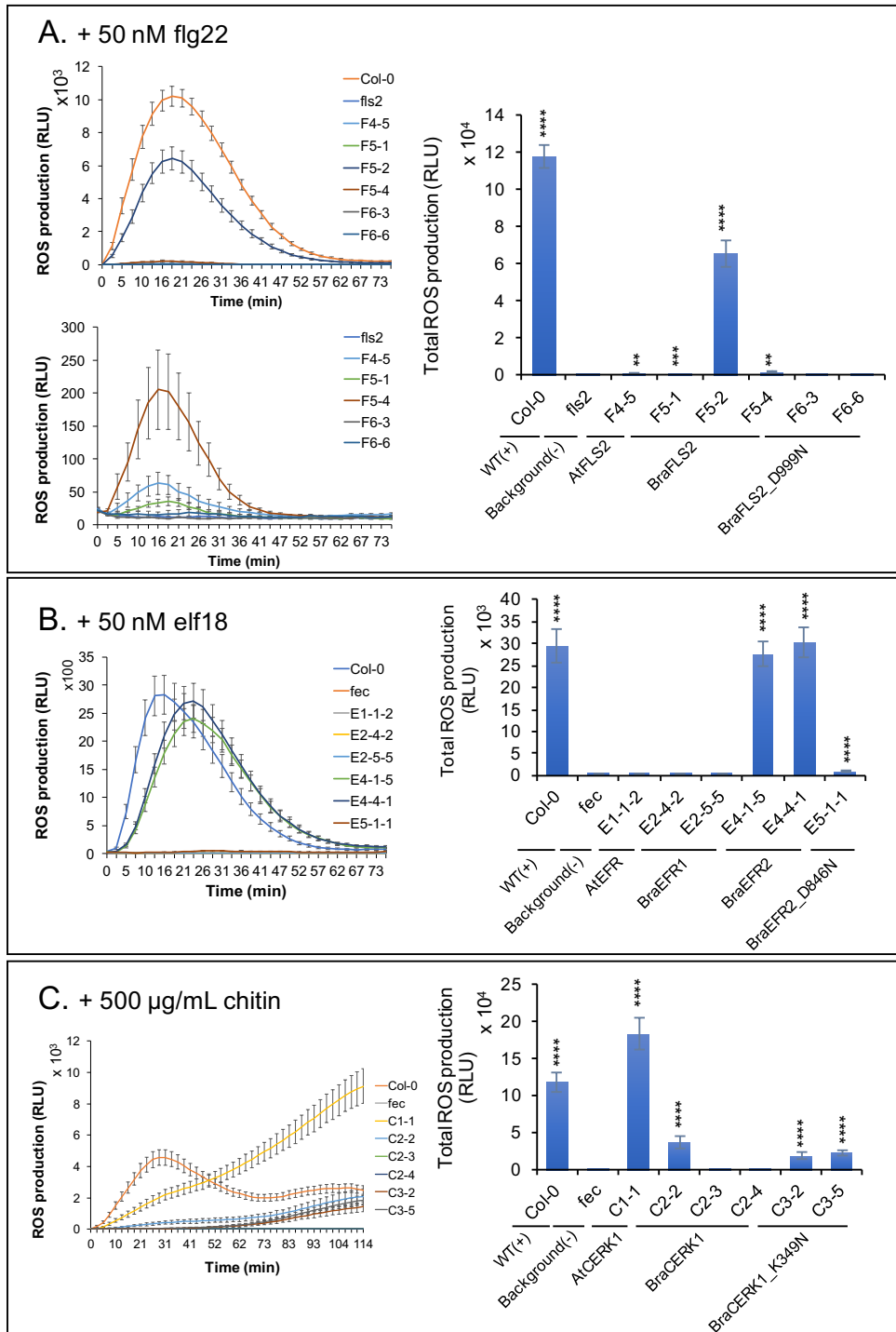
Figure 10 | PAMP-induced ROS production in transgenic *PRR* overexpressing lines

Leaves for assay were collected from 5-week-old Col-0, transgenic background plant *fec* and *fls2*, and *Arabidopsis* transgenic lines over-expressing *AtPRR*s, *BraPRR*s and *BraPRR*s dead kinase version fused with *6xHA* tag. After keeping on water in a 96-well plate overnight, leaf discs were challenged with 50 nM flg22 **(A)**, 50 nM elf18 **(B)** and 500 µg/mL chitin **(C)** before measurement. For each condition, 16 or 24 leaf discs were collected. ROS production (Relative Light Unit) was measured by chemiluminescence of oxidized luminol. Kinetic and total ROS production was measured for 75 minutes in three biological replicates ± standard error **(A)** and **(B)** or for 114 minutes in 2 biological replicates ± standard error **(C)**. Asterisks indicate significant differences compared to transgenic background plant *fec* or *fls2* by Student's T-test. ****: $p < 0.0001$ ***: $0.0001 < p < 0.001$ **: $0.001 < p < 0.01$ *: $0.01 < p < 0.05$ ns: $p \geq 0.05$.

Functional complementation in SGI assay and oxidative burst assay correlated with transgene expression.

To confirm whether the functional complementation correlated with transgene expression in *fls2* or *fec* mutant, the expression of transgenes was detected using CAPS analysis and *PRR-HA* amplification with special primers.

According to CAPS analysis, transgenes were correctly expressed in correlative transgenic lines. The transgenes of *AtPRR* transgenic lines were exactly as same as the gene from Col-0, and differed from the transgenes of *BraPRR* and transgenic *BraPRR* dead-kinase lines **[Figure 11]**. Both 223 nt PCR products of *FLS2* CAPS from Col-0 and from *AtFLS2* transgenic lines were digested into 87 nt and 136 nt fragments by *Cla*I. Conversely, *BraFLS2* CAPS was digested into 40 nt and 183 nt fragments by *Cla*I **[Figure 11A]**. For *EFR* transgenic lines, 656 nt CAPS from *AtEFR* were digested into 152 nt, 343 nt and 162 nt fragments by *Pst*I and *Eco*RI, but 659 nt CAPS from *BraEFR1* were digested into 94 nt and 565 nt fragments by *Eco*RI. 644 nt CAPS from *BraEFR2* could not be digested either by *Pst*I or *Eco*RI **[Figure 11B]**. For *CERK1* transgenic lines, 281 nt CAPS from *AtCERK1* could not be digested by *Eco*RI, but *BraCERK1* CAPS was digested by *Eco*RI into 85 nt and 196 nt fragments **[Figure 11C]**. As shown in results, transgenes of *BraFLS2, BraEFR1, BraEFR2* and *BraCERK1* were correctly expressed in correlative transgenic lines.

Then using transgenic *PRR-HA* fragment to analyze the expression level of transgenes, in *FLS2* transgenic lines, *AtFLS2*, *BraFLS2* and *BraFLS2_D999N* were expressed, although at a low level except in one of *BraFLS2_D999N* line F3-6, indicating that the complementation in SGI assay and oxidative burst assay was due to expression of transgene *AtFLS2* and *BraFLS2*. Moreover, although *BraFLS2_D999N* gene was expressed in F6-3 and F6-6, ROS burst was not induced,

indicating that kinase activity of BraFLS2 was required for ROS response. On the other hand, relatively high expression level of *BraFLS2_D999N* in F6-6 line conferred gain of flg22 perception and processed the seedling growth inhibition **[Figure 11A] [Figure 9A]**. In *EFR* transgenic lines, *BraEFR2* and *BraEFR2_D846N* were obviously well expressed in transgenic lines. In contrast, *AtEFR* and *BraEFR1* seemed to be expressed in an extremely low level **[Figure 11B]**. The results suggested that the expression of *BraEFR2* and *BraEFR2_D846N* were correlative to gain of elf18 perception in SGI assay and in the oxidative burst assay. But unlike *FLS2*, low expression of *AtEFR* seemed to be unable to trigger seedling growth inhibition and the oxidative burst. Likewise, it was difficult to confirm whether the immune behaviors in *BraEFR1* transgenic lines were resulted from the low expression level or from non-functionality of BraEFR1. In *CERK1* transgenic lines, because the common forward primer from CERK1 fragment mismatched 3 bases to target *AtCERK1*, it was off-target and failed in *AtCERK1* amplification. However, *BraCERK1* and *BraCERK1_K349N* were successfully amplified in *BraCERK1* transgenic line C2-2 and *BraCERK1_K349N* transgenic lines C3-2 and C3-5, which were sensitive to chitin and produced ROS burst. Non-responsive *BraCERK1* transgenic lines C2-3 and C2-4 did not seem to express *BraCERK1*, or they expressed *BraCERK1* in an extremely low level **[Figure 11C]**.
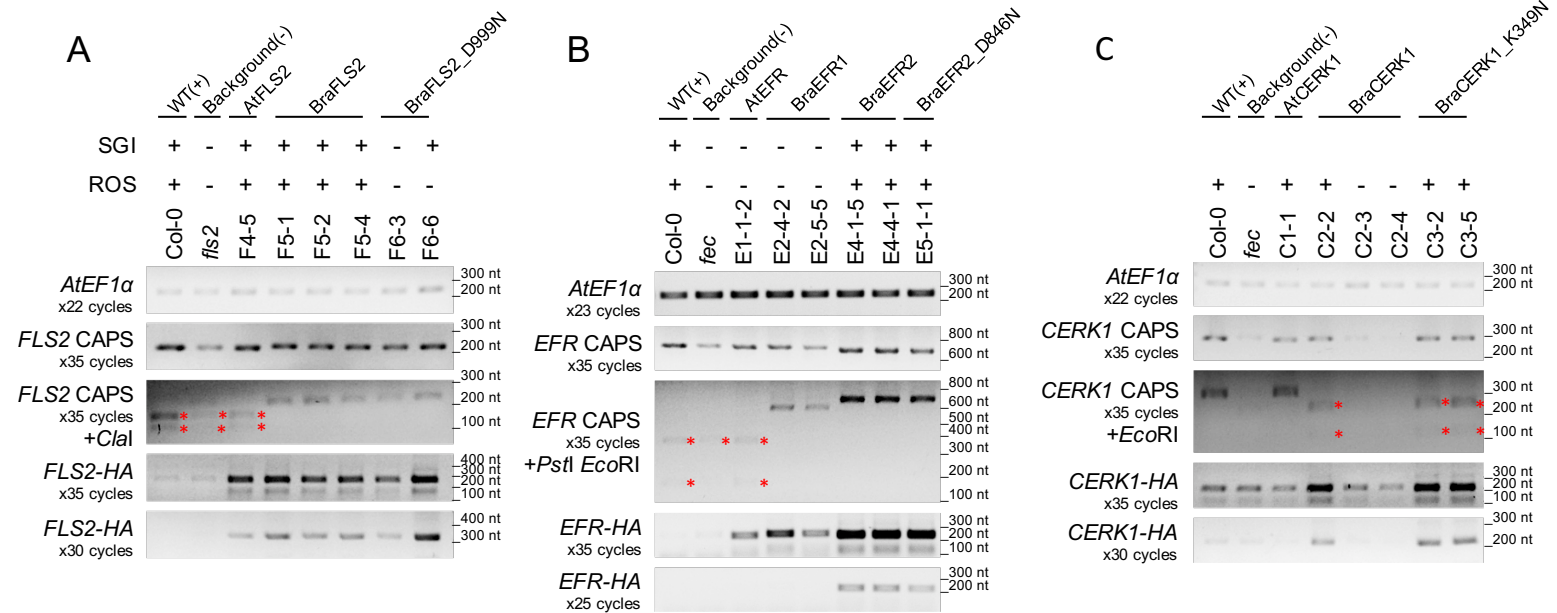
Figure 11 | Expression of transgenes in transgenic *PRR* expressing lines

Four plants of 14-day-old seedling from Col-0, *fec* and transgenic *EFR* expressing lines germinating on solid MS medium for 4 days and growing in liquid MS medium for an additional 10 days under LD condition **(B)** and one leaf disc per plant from eight different 5-week-old plants of each Col-0, *fec*, *fls2*, transgenic *CERK1* or *FLS2* expressing lines growing in soil under SD condition **(A)** and **(C)** were collected for RNA extraction. RT-PCR products were resolved on 2% agarose. *PRR* CAPS was digested by indicated enzymes for 1 hour then resolved on 2% agarose. Red asterisks indicate the presence of band.

In conclusion, Chinese cabbage was able to perceive several PAMPs, for example flg22, elf18, chitin, and induced transcriptional reprogramming. Flg22, elf18 and chitin triggered the oxidative burst in Chinese cabbage which is slightly different to the responses in Col-0.

These differences were probably due to the distinctions of protein sequences between BraPRR and AtPRR. Thus, the *B. rapa* synetic orthologs of *AtPRR*s were selected as *BraPRR* candidates. Comparative genomic analysis showed that BraPRRs shared high identity with AtPRRs in protein sequences. Between *BraFLS2* candidates (Bra017563 and Bra022032), only Bra017563 was expressed in *B. rapa* organs. Both two *BraEFR* candidates (Bra006560 and Bra002305) and unique *BraCERK1* candidate (Bra031293) were expressed in *B. rapa* organs. However, except BraCERK1 candidate, *BraFLS2* candidate Bra017563 and *BraEFR* candidates were expressed at low level in the leaves of Chinese cabbage cultivar "Norang kimchi baechu" during 6-week-growth. Hence, 4 candidate genes, Bra017563 called *BraFLS2*, Bra006560 called *BraEFR1*, Bra002305 called *BraEFR2* and Bra031293 called *BraCERK1*, were cloned as well as *AtFLS2*, *AtEFR*, *AtCERK1* and their dead-kinase versions.

Via transient expression in *N. benthamiana*, BraFLS2-YFP, BraEFR1-YFP, BraEFR2-YFP, and BraCERK1-YFP were localized at plasma membrane as same as AtFLS2. BraFLS2 mediated flg22-triggered endocytosis, BraEFR2 induced elf18-triggered oxidative burst and BraCERK1 led to chitin-independent cell death in *N. benthamiana*.

Via functional complementation analysis, the expression of transgene *BraFLS2*, *BraEFR2* and *BraCERK1* in *Arabidopsis fls2* or *fec* mutant conferred gains of flg22, elf18 and chitin responsiveness, respectively, demonstrating that *BraFLS2*, *BraEFR2* and *BraCERK1* probably function as PRR in Chinese cabbage **[Figure 12]**.
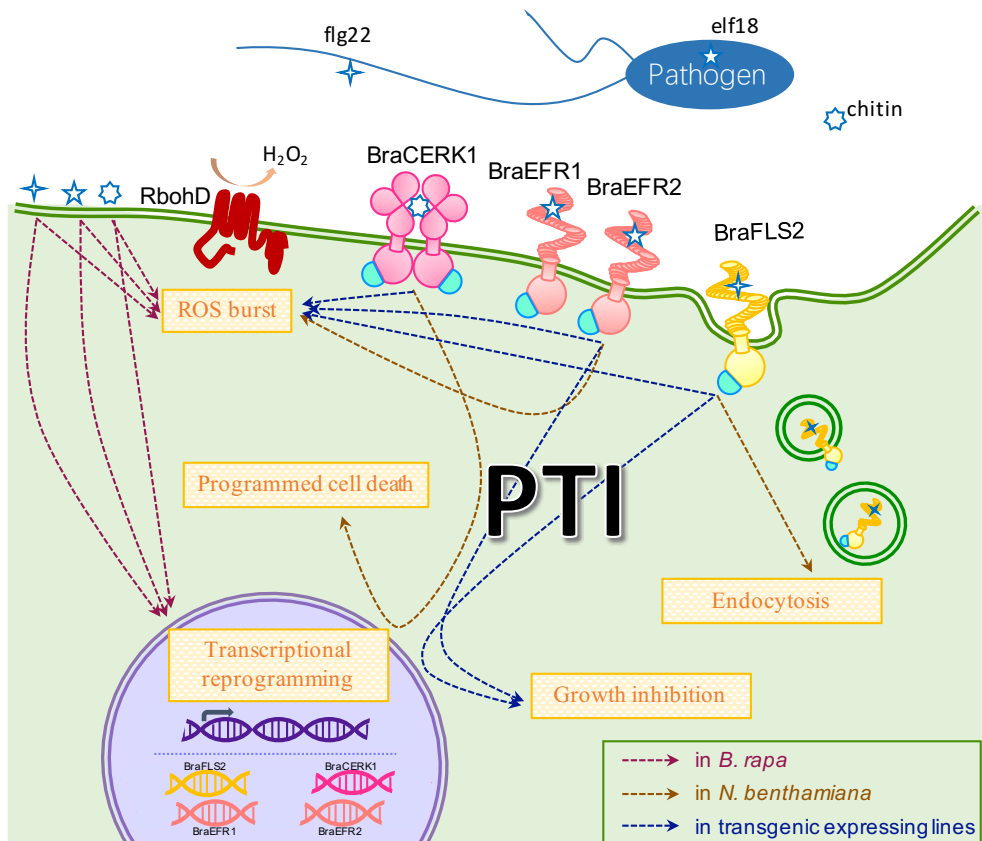
Figure 12 | Defense responses triggered by BraPRRs in this study

In Chinese cabbage, several PAMPs, flg22, elf18, chitin, could be perceived and induced transcriptional reprogramming or the oxidative burst. Putative flg22, elf18 and chitin sensing receptors *BraFLS2* (Bra017563), *BraEFR1* (Bra006560), *BraEFR2* (Bra002305) and *BraCERK1* (Bra031293) were identified and cloned. In *N. benthamiana* transiently expressing these putative *BraPRR*s, BraPRR proteins were localized at plasma membrane. BraFLS2 mediated flg22-triggered endocytosis. BraEFR2 induced elf18-triggered oxidative burst, but BraEFR1 could not induce ROS burst upon elf18 treatment. BraCERK1 led to cell death without chitin elicitation. In transgenic *PRR* expressing lines, transgenic BraFLS2, BraEFR2 induced PAMP-triggered seedling growth inhibition and both as well as BraCERK1 induced PAMP-triggered ROS burst, demonstrating that BraFLS2, BraEFR2 and BraCERK1 probably function as PRR in Chinese cabbage. BraEFR1 will need to be further tested.

DISCUSSION

The repertoire of PAMP-perception in Chinese cabbage

Comparative genomic analysis revealed the presence of several putative homologs for known *PRR*s in *B. rapa* genome **[Table 1]**, suggesting that Chinese cabbage was able to detect several PAMPs, for example, chitin, elf18, flg22, LPS and PGN. flg22, elf18 and chitin-responsiveness was well investigated by defense marker gene *BraNHL10* expression assay **[Figure 1]** and by the kinetic and dose-dependent oxidative burst assay **[Figure 2]**. However, LPS and PGN perceptions were rarely revealed via monitoring the regulation of *BraNHL10* expression **[Figure 1B and C]**. It was probably due to the inappropriate time points established in this assay. In previous studies, PTI marker genes *FRK1* and *GST1* were induced in *A. thaliana* seedling 4 h after LPS treatment **(Ranf et al., 2015)**, and PGN induced *FRK1* gene expression in *Arabidopsis* 6 h posttreatment **(Willmann et al., 2011)**, suggesting that the time points of 30, 60 and 180 min in this assay might be insufficient to trigger obvious marker gene expression.

Interestingly, no homolog of *CORE* or *CSPR* was found in *B. rapa* genome **[Table 1]**, but upon CSP22 exposure, a slight upregulation of two to six-fold in 30 min, compared to the control, was always observed in several repeats of quantitative assay **[Figure 1D]**, suggesting that the existence of CSP22-responsive receptor in Chinese cabbage.

Divergence in the expression of two *BraFLS2* candidates

Only one of two *BraFLS2* candidates, Bra017563 was expressed in the organs of Chinese cabbage and particularly at a high level in the leaves of 7-week-old cultivar Chiifu-401 **[Table 2]**. However, during 6-week-growth of cultivar Norang kimchi baechu, Bra017563 was expressed at a quite low level in the leaves **[Figure 4]**. It was unexpected because of the strong induction triggered by flg22 in defense marker gene *BraNHL10* expression **[Figure 1]** and in the oxidative burst assay **[Figure 2]**. Consistently, in the functional complementation analysis, the expression level of *BraFLS2* transgenes was irrelevant to the strength of immune responses, transgenic *BraFLS2* overexpressing line F5-2, which was shown the strongest inhibition of seedling growth **[Figure 9]** and the strongest production of ROS **[Figure 10]** in response to flg22 among all *BraFLS2* transgenic lines, expressed transgene *BraFLS2* at a level as low as other lines **[Figure 11]**. Three hypotheses could be put forward to explain.

First, a low expression of *BraFLS2* gene was sufficient to induce effective immune responses in plant, so the expression level was strictly controlled by plant system, and the difference of response strength between *BraFLS2* transgenic lines was due to the impairment of immunity relevant genes which was caused by insertion of transgene. Previous studies demonstrated that *AtFLS2* was expressed in flowers, leaves, stems and roots of *Arabidopsis* at a low level compared to Actin **(Gómez-Gómez and Boller, 2000)**. The overexpression of *AtFLS2* cDNA driven by *CaMV* 35S promoter in Col-0 reduced the expression level of *FLS2* in some transgenic lines, suggesting co-suppression of endogenous *AtFLS2*. Moreover, the seedling growth inhibition was reduced in T2 plants which were from one of reduced *FLS2* expressing lines **(Gómez-Gómez and Boller, 2000)**, that might be able to understand the reduction of seedling growth inhibition in all transgenic *AtFLS2*

overexpressing lines **[Figure 9]**. Furthermore, overexpression of *AtFLS2* gene in tomato cell did not accumulate more AtFLS2 protein than the endogenous AtFLS2 in Arabidopsis **(Chinchilla et al., 2006)**. All these results suggest that overexpression of *FLS2* gene in plant was a risk and *BraFLS2* was probably performed in a similar way like *AtFLS2*. Interestingly, Col-0 background-transgenic 35S : *AtFLS2* line with the enhanced *AtFLS2* expression level was shown a strong immune responses, suggesting the alterations in *FLS2* expression were direct relevant to flg22 responses **(Gómez-Gómez and Boller, 2000)**, however, no evidence supported the directly correlation between *BraFLS2* expression level and flg22 triggered responses in this study, for example transgenic *BraFLS2* overexpressing line F5-1 and F5-2.

Second, the strong immune responses might be induced by another unknown flg22-responsive gene, which might be expressed at a higher level than Bra017563 and more sensitive to flg22 in transgenic lines.

Thirdly, Bra017563 might induce strong immune responses in Chinese cabbage because the native immune system was more effective and suitable than the system in Col-0, as previous studies suggested that BraBAK1, the AtBAK1 homolog in *B. rapa*, had stronger activity of auto-phosphorylation and trans-phosphorylation than AtBAK1 **(Rameneni et al., 2015; Wu et al., 2012)**.

The other *BraFLS2* candidate, Bra022031 was not expressed in any *B. rapa* organs **[Table 2]**. Comparative genomic analysis showed that it lost several functional domains **[Figure 3B]**, indicating that Bra022032 was likely silenced via natural selection because of the loss of flg22-binding function and miscontribution of transmembrane domain.

Functionality between two *BraEFR* candidates

In response to elf18, ROS production was induced with a weaker strength in Chinese cabbage than in Col-0 **[Figure 2]**. Consistently, *AtEFR* transiently expressing line produced more ROS accumulation in *N. benthamiana* than *BraEFR2* transiently expressing line **[Figure 7]**, indicating that BraEFR2 was most likely less sensitive and less active than AtEFR. BraEFR2 shared 76.7% identity with AtEFR in protein sequence, suggesting that the difference between two proteins will be helpful in deciphering the activity of EFR.

On the other hand, the overexpression of *BraEFR2* in *Arabidopsis fec* mutant complemented elf18-responsive seedling growth inhibition **[Figure 9]** and ROS burst **[Figure 10]** up to the similar strength with the responses in Col-0, suggesting the potential to improve the immunity of Chinese cabbage via overexpressing *BraEFR2* or transgenic expression of *AtEFR*.

Unavoidably connected the expression level to the relatively weak immune responses observed in Chinese cabbage, both two *BraEFR* candidates were expressed at extremely low level in Chinese cabbage **[Table 2] [Figure 4]**. In addition, it was failed to clone *BraEFR1* gene from the genome of cultivar Norang kimchi baechu **[Appendix B]**. It was probably due to the low expression level of *BraEFR1*. However, it was also probably due to inexistence of *BraEFR1* in the genome of cultivar Norang kimchi baechu which is commercial and generated by hybridization. Indeed, BraEFR1 specific sequences could be amplified from Chiifu-401 genomic DNA (Cecile Segonzac, personal communication).

Via transient expression in *N. benthamiana*, although BraEFR1 was well expressed in leaves and localized at plasma membrane as well as characterized PRRs in plant **[Figure 6]**, BraEFR1 did not contribute to ROS burst **[Figure 7]**, indicating BraEFR1 most likely did not function for the immunity. Non-functionality of

BraEFR1 would be further confirmed in functional complementation assay. Unfortunately, *BraEFR1* in *fec* mutant was not expressed at a significant level **[Figure 11]** and did not induce any significant response in seedling growth inhibition **[Figure 9]** and the oxidative burst **[Figure 10]** upon elf18 treatment. These results made it difficult to judge the functionality of BraEFR1. In order to find well expressing lines of *BraEFR1* and *AtEFR*, T2 plants of transgenic *AtEFR* overexpressing lines E1-1, E1-2 and E1-3, and transgenic *BraEFR1* overexpressing lines E2-3, E2-4 and E2-5 were tested by SGI assay, but none of them was shown a significant inhibition of seedling growth upon elf18 dose change **[data not shown]**. The selection of transgenic lines is still in progress.

BraCERK1: the PTI dogma breaker

In this study, chitin was from the shell of crab that more or less affected chitin responsive immune responses, due to the distinction in the degree of polymerization (DP). The structures and properties of chitin rely on DP. Chitin oligosaccharides, which are released from fungi and could be recognized by plants, are with DP=6-8 **(Stacey and Shibuya, 1997)**. Whereas the product of chitin obtained through the industrial and chemical treatments often varies in DP.

Nevertheless, chitin triggered strong expression of defense marker gene *BraNHL10* **[Figure 1]** and ROS production **[Figure 2]**. *BraCERK1*, the unique syntenic ortholog of *AtCERK1* in *B. rapa* genome, was expressed at high level both in Chiifu-401 and Norang kimchi baechu cultivars, differing from the low expression of *BraFLS2* and *BraEFR*s **[Table 2] [Figure 4]**. BraCERK1 protein sequence shared high identity with AtCERK1 **[Figure 3E] [Table 3]**, and induced cell death in *N. benthamiana* as well as AtCERK1 **(Pietraszewska-Bogiel et al., 2013) [Figure 8]**.

Generally, PTI events were not deemed to induce hypersensitive response in plant. One hypothesis states here that overexpressed BraCERK1 or AtCERK1 might aggregate at plasma membrane and dimerize with each other or with NbCERK1 to become activated and transport excessive immune signals, finally resulting in cell death. Overexpression of *BraCERK1* in *Arabidopsis fec* mutant also contributed an abnormal ROS production in response to chitin. Plant seemed to lose negative control to inhibit that abnormal ROS production and lead to a constant amplified response **[Figure 10]**.

ROS is widely acknowledged that it is not only an important defense signal but also harmful gas to plant cell itself. It is also deemed to be involved in programmed cell death **(Van Breusegem and Dat, 2006)**. Plant has a sophisticated negative feedback loop to balance ROS contribution, resulting in a regular decrease of ROS production after reaching the peak of response as shown in the oxidative burst assay in response to flg22 or elf18 in Chinese cabbage **[Figure 2]**, in *N. benthamiana* **[Figure 7]** or in transgenic FLS2 and EFR overexpressing lines **[Figure 10]**. However, these behaviors of *BraCERK1* will contribute to redefining the PTI events and deciphering the defense mechanism of LysM-RLK receptors.

Kinase activity of BraFLS2, BraEFR2 and BraCERK1 for immune responses

Regretfully, it is difficult to indicate whether BraFLS2 kinase activity is indispensable for BraFLS2-mediated endocytosis in *N. benthamiana*, because *BraFLS2* kinase dead version *BraFLS2_D999N* line was not examined in *N. benthamiana* via transient expression assay **[Figure 6]**. However, in *Arabidopsis* transgenic lines, the impaired kinase of BraFLS2 reduced BraFLS2-mediated

seedling growth inhibition **[Figure 9]** and reduced ROS production **[Figure 10]**, indicating that *BraFLS2* kinase activity was indispensable for flg22-triggered ROS burst but only influential for flg22-triggered seedling growth inhibition.

The other receptor from LRR-RLK family, transiently expressing *BraEFR2_D846N* in *N. benthamiana* did not allow elf18-triggered ROS production **[Figure 7]**, however, transgenic overexpressing *BraEFR2_D846N* in *Arabidopsis fec* mutant induced both seedling growth inhibition **[Figure 9]** and oxidative burst **[Figure 10]** in response to elf18. Previous studies indicated that BAK1 is involved in the signaling of both growth and development **(Li et al., 2002; Nam and Li, 2002)**, and plant innate immunity as a co-receptor by forming a PAMP-induced complex with PRR, for example in FLS2 and EFR signaling in *Arabidopsis* **(Chinchilla et al., 2007)**. The *bak1* mutant plants decreased the responses to flg22 and elf18 **(Chinchilla et al., 2007)**. Furthermore, BraBAK1 and AtBAK1 were demonstrated to have strong kinase activity, whereas little evidence could support FLS2 has a strong kinase activity, both in Chinese cabbage or in *Arabidopsis*, except one putative transphosphorylation site found in AtFLS2 protein **(Rameneni et al., 2015; Wu et al., 2012)**. Therefore, the functional complementation in *Arabidopsis* transgenic *BraFLS2_D999N* and *BraEFR2_D846N* overexpressing lines were probably contributed from the kinase activity of co-receptor like AtBAK1. As is known to all, elf18 sensing receptor EFR does not exist in *N. benthamiana*, hypothesizing that there is not effective co-receptor that could contribute to the kinase activity of BraEFR2_D846N. Probably, the divergence of intracellular signaling pathways between *Brassicaceae* and *Solanaceae* family led that transient expression of BraEFR2_D846N could not produce ROS in response to elf18 in *N. benthamiana*.

BraCERK1_K349N could mediate immune responses both in *N. benthamiana*

[Figure 8] and in *Arabidopsis* transgenic lines **[Figure 10]**. It was probably due to the retaining of kinase activity, because the right ATP-binding site K348 was not mutated **[Figure 3E]**. Although the kinase activity seems to retain, the mutant of one amino acid K349 in kinase domain reduced the strength of immune responses in cell death **[Figure 8]** and oxidative burst **[Figure 10]**, indicating that the kinase activity of BraCERK1 is crucial to immunity.

Diverse degrees of immune responses from T2 transgenic plants

The screening of T3 homozygous lines is still in progress, therefore T2 plants of *FLS2* and *CERK1* transgenic expressing lines were examined in functional complementation analysis. Although PAMP-responsiveness was gained via transgene expression in T2 lines, the heterozygous phenotypes in T2 lines reduced the strength of responses in SGI assay and in the oxidative burst assay. They also affected the expression level of transgenes, because only approximately ⅓ plants responded to PAMP treatment and expressed transgenes.

In further study, T3 homozygous lines will be screened after examining the expression level of transgene and protein. The T3 homozygous with appropriate expression level of protein will be used.

The conserved and sophisticated immune system of plant

Although treated by diverse PAMPs, mediated by distinct PRRs, performed in various species (*B. rapa*, *N. benthamiana* or *Arabidopsis*), the intracellular signaling pathway of PTI was conserved and controlled. The normal immune responses triggered in foreign *FLS2* or *EFR* overexpressing lines, and the suppression of the

overexpression of native *EFR*, all these behaviors indicated that plants have a sophisticated system to protect their own immunity. The convergence of signaling pathway demonstrated the evolutionary convergence in the immune system or mechanism of plants, and the divergence of PRR and downstream components suggested the dynamic of plants in response to variable environmental conditions.

REFERENCES

Albrecht C, Boutrot F, Segonzac C, Schwessinger B, Gimenez-Ibanez S, Chinchilla D, Rathjen JP, de Vries SC, Zipfel C. (2012). Brassinosteroids inhibit pathogen-associated molecular pattern-triggered immune signaling independent of the receptor kinase BAK1. *Proc. Natl. Acad. Sci. USA* 109, 303–308.

Beck M, Wyrsch I, Strutt J, Wimalasekera R, Webb A, Boller T, Robatzek S. (2014). Expression patterns of flagellin sensing 2 map to bacterial entry sites in plant shoots and roots. *J. Exp. Bot*. 65(22):6487-98.

Böhm H, Albert I, Fan L, Reinhard A, Nürnberger T. (2014). Immune receptor complexes at the plant cell surface. *Curr. Opin. Plant Biol*. 20:47-54.

Buscaill P, Chandrasekar B, Sanguankiattichai N, Kourelis J, Kaschani F, Thomas EL, Morimoto K, Kaiser M, Preston GM, Ichinose Y, van der Hoorn RAL. (2019). Glycosidase and glycan polymorphism control hydrolytic release of immunogenic flagellin peptides. *Science* 364(6436).

Cai R, Lewis J, Yan S, Liu H, Clarke CR, Campanile F, Almeida NF, Studholme DJ, Lindeberg M, Schneider D, Zaccardelli M, Setubal JC, Morales-Lizcano NP, Bernal A, Coaker G, Baker C, Bender CL, Leman S, Vinatzer BA. (2011). The plant pathogen *Pseudomonas syringae* pv. *tomato* is genetically monomorphic and under strong selection to evade tomato immunity. *PLOS Pathog*. 7:e1002130.

Che FS, Nakajima Y, Tanaka N, Iwano M, Yoshida T, Takayama S, Kadota I, Isogai A. (2000). Flagellin from an incompatible strain of *Pseudomonas avenae* induces a resistance response in cultured rice cells. *J. Biol. Chem.* 275:32347–56.

Cheng F, Liu S, Wu J, Fang L, Sun S, Liu B, Li P, Hua W, Wang X. (2011). BRAD, the genetics and genomics database for *Brassica* plants. *BMC Plant Biol*. 11:136.

Chinchilla D, Bauer Z, Regenass M, Boller T, Felix G. (2006). The *Arabidopsis* receptor kinase FLS2 binds flg22 and determines the specificity of flagellin perception. *Plant Cell* 18, 465–476.

Chinchilla D, Zipfel C, Robatzek S, Kemmerling B, Nürnberger T, Jones JD, Felix G, Boller T. (2007). A flagellin-induced complex of the receptor FLS2 and BAK1 initiates plant defence. *Nature* 448, 497–500.

Clough SJ, Bent AF. (1998). Floral dip: a simplified method for *Agrobacterium*-mediated transformation of *Arabidopsis thaliana*. *Plant J*. 16(6):735-43.

Cook DE, Mesarich CH, Thomma BP. (2015). Understanding plant immunity as a surveillance system to detect invasion. *Annu. Rev. Phytopathol*. 53:541-63.

Dangl JL, Horvath DM, Staskawicz BJ. (2013). Pivoting the plant immune system from dissection to deployment. *Science* 341:746–51.

Dodds PN, Rathjen JP. (2010). Plant immunity: towards an integrated view of plant-pathogen interactions. *Nat. Rev. Genet.* 11:539-548.

Dunning FM, Sun W, Jansen KL, Helft L, Bent AF. (2007). Identification and mutational analysis of *Arabidopsis* FLS2 leucine-rich repeat domain residues that contribute to flagellin perception. *Plant Cell* 19, 3297–3313.

Erbs G, Silipo A, Aslam S, de Castro C, Liparoti V, Flagiello A, Pucci P, Lanzetta R, Parrilli M, Molinaro A, Newman MA, Cooper RM. (2008). Peptidoglycan and muropeptides from pathogens *Agrobacterium* and *Xanthomonas* elicit plant innate immunity: structure and activity. *Chem. Biol*. 15:438–448.

Erbs G, Newman MA. (2012). The role of lipopolysaccharide and peptidoglycan, two glycosylated bacterial microbe-associated molecular patterns (MAMPs), in plant innate immunity. *Mol. Plant Pathol*. 13(1):95-104.

Felix G, Duran JD, Volko S, Boller T. (1999). Plants have a sensitive perception system for the most conserved domain of bacterial flagellin. *Plant J*. 18, 265–276.

Felix G, Boller T. (2003). Molecular sensing of bacteria in plants. The highly conserved RNA-binding motif RNP-1 of bacterial cold shock proteins is recognized as an elicitor signal in tobacco. *J. Biol. Chem*. 278(8):6201-8.

Force A, Lynch M, Pickett FB, Amores A, Yan YL, Postlethwait J. (1999). Preservation of duplicate genes by complementary, degenerative mutations. *Genetics* 151(4):1531-45.

Franco-Orozco B, Berepiki A, Ruiz O, Gamble L, Griffe LL, Wang S, Birch PRJ, Kanyuka K, Avrova A. (2017). A new proteinaceous pathogen-associated molecular pattern (PAMP) identified in Ascomycete fungi induces cell death in *Solanaceae*. *New Phytol*. 214(4):1657-1672.

Furukawa T, Inagaki H, Takai R, Hirai H, Che FS. (2014). Two distinct EF-Tu epitopes induce immune responses in rice and *Arabidopsis*. *Mol. Plant-Microbe Interact*. 27(2):113-24.

Gimenez-Ibanez S, Hann DR, Ntoukakis V, Petutschnig E, Lipka V, Rathjen JP. (2009). AvrPtoB targets the LysM receptor kinase CERK1 to promote bacterial virulence on plants. *Curr. Biol. CB* 19: 423– 429.

Gómez-Gómez L, Felix G, Boller T. (1999). A single locus determines sensitivity to bacterial flagellin in *Arabidopsis thaliana*. *Plant J*. 18(3):277-84.

Gómez-Gómez L, Boller T. (2000). FLS2: an LRR receptor-like kinase involved in the perception of the bacterial elicitor flagellin in *Arabidopsis*. *Molecular Cell* 5: 1003– 1011.

Gross A, Kapp D, Nielsen T, Niehaus K. (2005). Endocytosis of *Xanthomonas campestris pathovar campestris* lipopolysaccharides in non-host plant cells of *Nicotiana tabacum*. *New Phytol*. 165(1):215-26.

Gust AA, Biswas R, Lenz HD, Rauhut T, Ranf S, Kemmerling B, Gotz F, Glawischnig E, Lee J, Felix G, Nürnberger T. (2007). Bacteria-derived peptidoglycans constitute pathogen-associated molecular patterns triggering innate immunity in Arabidopsis. *J. Biol. Chem*. 282:32338–32348.

Hann DR, Rathjen JP. (2007). Early events in the pathogenicity of *Pseudomonas syringae* on *Nicotiana benthamiana*. *Plant J*. 49, 607–618.

Häweker H, Rips S, Koiwa H, Salomon S, Saijo Y, Chinchilla D, Robatzek S, von Schaewen A. (2010). Pattern recognition receptors require N-glycosylation to mediate plant immunity. J. Biol. Chem. 285(7):4629-36.

Heese A, Hann DR, Gimenez-Ibanez S, Jones AM, He K, Li J, Schroeder JI, Peck SC, Rathjen JP. (2007). The receptor-like kinase SERK3/BAK1 is a central regulator of innate immunity in plants. *Proc. Natl. Acad. Sci. USA* 104, 12217–12222.

Jones JDG, and Dangl JL. (2006). The plant immune system. *Nature* 444:323–29.

Kadota Y, Sklenar J, Derbyshire P, Stransfeld L, Asai S, Ntoukakis V, Jones J, Shirasu K, Menke F, Jones A, Zipfel C. (2014). Direct regulation of the

NADPH oxidase RBOHD by the PRR-associated kinase BIK1 is required for ROS burst and plant immunity. *Mol. Cell* 54, 43–55.

Kunze G, Zipfel C, Robatzek S, Niehaus K, Boller T, Felix G. (2004). The N terminus of bacterial elongation factor Tu elicits innate immunity in *Arabidopsis* plants. *Plant Cell* 16:3496–507.

Lacombe S, Rougon-Cardoso A, Sherwood E, Peeters N, Dahlbeck D, van Esse P, Smoker M, Rallapalli G, Thomma B, Staskawicz B, Jones J, Zipfel C. (2010). Interfamily transfer of a plant pattern recognition receptor confers broad-spectrum bacterial resistance. *Nat. Biotechnol*. 28:365-369.

Li J, Wen J, Lease KA, Doke JT, Tax FE, Walker JC. (2002). BAK1, an Arabidopsis LRR receptor-like protein kinase, interacts with BRI1 and modulates brassinosteroid signaling. *Cell* 110, 213–222.

Li L, Li M, Yu L, Zhou Z, Liang X, Liu Z, Cai G, Gao L, Zhang X, Wang Y, Chen S, Zhou JM. (2014). The FLS2-associated kinase BIK1 directly phosphorylates the NADPH oxidase RbohD to control plant immunity. *Cell Host Microbe* 15(3):329-38.

Li B, Meng X, Shan L, He P. (2016). Transcriptional Regulation of Pattern Triggered Immunity in Plants. *Cell Host Microbe* 19(5):641-50.

Liu T, Liu Z, Song C, Hu Y, Han Z, She J, Fan F, Wang J, Jin C, Chang J, Zhou JM, Chai J. (2012). Chitin-induced dimerization activates a plant immune receptor. *Science* 336: 1160– 1164.

Lu D, Wu S, Gao X, Zhang Y, Shan L, He P. (2010). A receptor-like cytoplasmic kinase, BIK1, associates with a flagellin receptor complex to initiate plant innate immunity. *Proc. Natl. Acad. Sci. USA* 107, 496–501.

Macho AP, Zipfel C. (2014). Plant PRRs and the activation of innate immune signaling. *Mol. Cell* 54(2):263-72.

Marutani M, Taguchi F, Shimizu R, Inagaki Y, Toyoda K, Shiraishi T, Ichinose Y. (2005). Flagellin from *Pseudomonas syringae* pv. *tabaci* induced *hrp*-independent HR in tomato. *J. Gen. Plant Pathol.* 71: 289–295.

Miya A, Albert P, Shinya T, Desaki Y, Ichimura K, Shirasu K, Narusaka Y, Kawakami N, Kaku H, Shibuya N. (2007). CERK1, a LysM receptor kinase, is essential for chitin elicitor signaling in *Arabidopsis*. *Proc. Natl. Acad. Sci. USA* 104:19613–18.

Monaghan J, Zipfel C. (2012). Plant pattern recognition receptor complexes at the plasma membrane. *Curr. Opin. Plant Biol.* 15(4):349-57.

Nam KH, Li J. (2002). BRI1/BAK1, a receptor kinase pair mediating brassinosteroid signaling. *Cell* 110, 203–212.

Petutschnig EK, Jones AM, Serazetdinova L, Lipka U, Lipka V. (2010). The lysin motif receptor-like kinase (LysM-RLK) CERK1 is a major chitin-binding protein in *Arabidopsis thaliana* and subject to chitin-induced phosphorylation. *J. Biol. Chem*. 285, 28902–28911.

Pietraszewska-Bogiel A, Lefebvre B, Koini MA, Klaus-Heisen D, Takken FL, Geurts R, Cullimore JV, Gadella TW. (2013). Interaction of *Medicago truncatula* lysin motif receptor-like kinases, NFP and LYK3, produced in *Nicotiana benthamiana* induces defence-like responses. *PLoS One* 8(6):e65055.

Rameneni JJ, Lee Y, Dhandapani V, Yu X, Choi SR, Oh MH, Lim YP. (2015). Genomic and Post-Translational Modification Analysis of Leucine-Rich-Repeat Receptor-Like Kinases in *Brassica rapa*. *PLoS One* 10(11):e0142255.

Ranf S, Gisch N, Schäffer M, Illig T, Westphal L, Knirel YA, Sánchez-Carballo PM, Zähringer U, Hückelhoven R, Lee J, Scheel D. (2015). A lectin S-domain receptor kinase mediates lipopolysaccharide sensing in *Arabidopsis thaliana*. *Nat. Immunol*. 16(4):426-33.

Robatzek S, Chinchilla D, Boller T. (2006). Ligand-induced endocytosis of the pattern recognition receptor FLS2 in *Arabidopsis*. *Genes Dev*. 20, 537–542.

Robatzek S, Bittel P, Chinchilla D, Köchner P, Felix G, Shiu SH, Boller T. (2007). Molecular identification and characterization of the tomato flagellin receptor LeFLS2, an orthologue of *Arabidopsis* FLS2 exhibiting characteristically different perception specificities. *Plant Mol. Biol.* 64, 539–547.

Shibuya, N. and Minami, E. (2001). Oligosaccharide Signaling for Defense Responses in Plant. *Physiol. Mol. Plant Pathol*. 59, 223-233.

Shimizu T, Nakano T, Takamizawa D, Desaki Y, Ishii-Minami N, Nishizawa Y, Minami E, Okada K, Yamane H, Kaku H, Shibuya N. (2010). Two LysM receptor molecules, CEBiP and OsCERK1, cooperatively regulate chitin elicitor signaling in rice. *Plant J*. 64: 204– 214.

Rastogi S, Liberles DA. (2005). Subfunctionalization of duplicated genes as a transition state to neofunctionalization. *BMC Evol. Biol*. 5:28.

Smith JM, Salamango DJ, Leslie ME, Collins CA, Heese A. (2014). Sensitivity to Flg22 is modulated by ligand-induced degradation and de novo synthesis of the endogenous flagellin-receptor FLAGELLIN-SENSING2. *Plant Physiol*. 164, 440–454.

Stacey G and Shibuya N, (1997). Chitin recognition in rice and legumes. *Plant Soil* 194: 161–169.

Taguchi F, Shimizu R, Inagaki Y, Toyoda K, Shiraishi T, Ichinose Y. (2003). Post-translational modification of flagellin determines the specificity of HR induction. *Plant Cell Physiol*. 44(3):342-9.

Takai R, Isogai A, Takayama S, Che FS. (2008). Analysis of flagellin perception mediated by flg22 receptor OsFLS2 in rice. *Mol. Plant-Microbe Interact*. 21(12):1635-42.

Tena G, Boudsocq M, Sheen J. (2011). Protein kinase signaling networks in plant innate immunity. *Curr. Opin. Plant Biol*. 14:519-529.

Tong C, Wang X, Yu J, Wu J, Li W, Huang J, Dong C, Hua W, Liu S. (2013). Comprehensive analysis of RNA-seq data reveals the complexity of the transcriptome in *Brassica rapa*. *BMC Genomics* 14:689.

Van Breusegem F, Dat JF. (2006). Reactive oxygen species in plant cell death. *Plant Physiol*. 141(2):384-90.

Wan J, Zhang XC, Neece D, Ramonell KM, Clough S, Kim SY, Stacey MG, Stacey G. (2008). A LysM receptor-like kinase plays a critical role in chitin signaling and fungal resistance in Arabidopsis. *Plant Cell* 20(2):471-81.

Wang X, Wang H, Wang J, Sun R, Wu J, Liu S, Bai Y, Mun JH, Bancroft I, Cheng F, Huang S, Li X, Hua W, Wang J, Wang X, et al. (2011). The genome of the mesopolyploid crop species *Brassica rapa*. *Nat. Genet*. 43(10):1035-9.

Willmann R, Lajunen HM, Erbs G, Newman M-A, Kolb D, Tsuda K, Katagiri F, Fliegmann J, Bono J-J, Cullimore JV *et al*. (2011). *Arabidopsis* lysin-motif proteins LYM1 LYM3 CERK1 mediate bacterial peptidoglycan sensing and immunity to bacterial infection. *Proc. Natl. Acad. Sci. USA*. 108: 19824-19829.

Winter D, Vinegar B, Nahal H, Ammar R, Wilson GV, Provart NJ. (2007). An "Electronic Fluorescent Pictograph" browser for exploring and analyzing large-scale biological data sets. *PLoS One* 2(8):e718.

Wu X, Oh MH, Kim HS, Schwartz D, Imai BS, Yau PM, Clouse SD, Huber SC. (2012). Transphosphorylation of *E. coli* proteins during production of recombinant protein kinases provides a robust system to characterize kinase specificity. *Front. Plant Sci*. 3:262.

Zhang J, Li W, Xiang T, Liu Z, Laluk K, Ding X, Zou Y, Gao M, Zhang X, Chen S, Mengiste T, Zhang Y, Zhou J-M. (2010). Receptor-like cytoplasmic kinases integrate signaling from multiple plant immune receptors and are targeted by a *Pseudomonas syringae* effector. *Cell Host Microbe* 7, 290–301.

Zipfel C, Kunze G, Chinchilla D, Caniard A, Jones JDG, Boller T, Felix G. (2006). Perception of the bacterial PAMP EF-Tu by the receptor EFR restricts *Agrobacterium*-mediated transformation. *Cell* 125: 749– 760.

Zipfel, C. (2014). Plant pattern-recognition receptors. *Trends Immunol*. 35(7):345-51.

APPENDICES

Appendix A | Primers list

	Gene name	Gene ID	CSP#		Sequence (5'→3')	Purpose
RT-PCR	*BraEF1α*	Bra006661	CS054	F	TACCTCCCAGGCTGATTGTG	Check gDNA contamination.
			CS055	R	CCAGTCAAGGTTGGTGGACC	Around 84 bp intron (gDNA 400bp/cDNA 316bp)
			CS012	F	TTCGCTCCTTCAGGGTTGAC	Reference gene
			CS013	R	TGCAGCCTTGGTGACCTTAG	
	BraNHL10	Bra017272	CS016	F	AACCTCTCAACGGTGCCTTC	Defense marker gene
			CS017	R	AACTCCGGCGATACTCTCCT	
	BraCYP81F2	Bra020459	CS020	F	GGGAACGGATACTGCAGCC	Defense marker gene
			CS021	R	TGTCCTCACCGTTGACTTTCT	
	BraMPK4	Bra000955	CS024	F	AACTGCTCCGAGTACACAGC	Defense marker gene
			CS025	R	GGATTGAACTTGACTGTCTCACG	
	BraWRKY33	Bra005104	CS026	F	CCTAAACCTCAGTCCACTCGA	Defense marker gene
			CS027	R	TTGGTGCTGAAGAAGGCTCT	
qRT-PCR	*BraEF1α*	Bra006661	CS064	F	TTGACGGGCGATCTGGAAAG	Reference gene (Bra006661)_1,184 F
			CS065	R	TCCCTAACAGCGAAACGACC	Reference gene (Bra006661)_1,331 R
	BraNHL10	Bra017272	CS058	F	TTCAACGCCGGAGAGTTACG	Defense marker gene
			CS059	R	TCCCCAAGCTTAAACCTAACCC	
			CS227	F	AGCCGCTCTTATCTTCTGGC	
			CS228	R	TTGTTAGGGTTGCGGACAGG	
	BraFLS2	Bra017563	CS245	F	TCACGTCAGCGATTTTGGGA	Test expression of *BraFLS2*
			CS246	R	AATCCCGAAGCTGAACACGT	
	BraCERK1	Bra031293	CS239	F	CGCGGTTGTCAAGATGAACC	Test expression of *BraCERK1*
			CS240	R	TCCCTAGCTCCGCCATCTTA	

Appendix A (*continued*)

	Gene name	Gene ID	CSP#		Sequence (5'→3')	Purpose
AtFLS2	*AtFLS2*	AT5G46330	CS199	F	ggtctcaAATGAAGTTACTCTCAAAGACCTTTTTG	Golden Gate cloning of *AtFLS2* _module 1
			CS200	R	ggtctcaCAAGTTCCTCAAGTTTGTGATGGA	
			CS201	F	ggtctcaCTTGACAGTCCTAACGGTGGG	Golden Gate cloning of *AtFLS2* _module 2
			CS202	R	ggtctcaGATCCAAGGACACCAAATGCG	(CS202: *Bsa*I removed)
			CS203	F	ggtctcaGATCTCTCTAGTAACAATCTCACTGGT	Golden Gate cloning of *AtFLS2* _module 3
			CS204	R	ggtctcaGTTTCGTCATCAGCTCCATCA	
			CS205	F	ggtctcaAAACAGAGGCCAACTTCGTTGA	Golden Gate cloning of *AtFLS2* _module 4
			CS206	R	ggtctcaCGAAAACTTCTCGATCCTCGTTACGA	(CS205: *Bsa*I removed)
BraFLS2	*BraFLS2*	Bra017563	CS207	F	ggtctcaAATGACTTCACTCTCAAAGACAACT	Golden Gate cloning of *BraFLS2* _module 1
			CS208	R	ggtctcaCAAGTTCTTCATGTTTGTGATTGACTG	
			CS209	F	ggtctcaCTTGACAGTGATAACAATGGGATTCA	Golden Gate cloning of *BraFLS2* _module 2
			CS210	R	ggtctcaGATCCAGAGAGACTAGATGCGT	
			CS211	F	ggtctcaGATCTCTCTTCTAACAATCTCACAGG	Golden Gate cloning of *BraFLS2* _module 3
			CS212	R	ggtctcaGTTTCGTCATCAGCTCCATCA	
			CS213	F	ggtctcaAAACGTAGACCAACTTCGGTGA	Golden Gate cloning of *BraFLS2* _module 4
			CS214	R	ggtctcaCGAACACTTCTAAATCACCATTACAATCTGG	(CS213: *Bsa*I removed)
			CS233	F	TCCCGATCGTGCATTGCAATCTGAAGCCGGCGAA	*BraFLS2* _module 3_D999N
			CS234	R	TTCGCCGGCTTCAGATTGCAATGCACGATCGGGA	Mutagenesis to make dead-kinase-version
AtEFR	*AtEFR*	AT5G20480	CS048	F	GGTCTCAAATGAAGCTGTCCTTTTCACTTG	Golden Gate cloning of *AtEFR* _module 1
			CS049	R	GGTCTCAAGAGATAAGATTTTGTCCAAGG	
			CS050	F	GGTCTCACTCTGGAACCATTCCTCATGACATCG	Golden Gate cloning of *AtEFR* _module 2
			CS051	R	GGTCTCAAGGTTTCACATTCCGCCATAAAGC	
			CS052	F	GGTCTCAACCTTCAAGGGTATACGACATCG	Golden Gate cloning of *AtEFR* _module 3
			CS053	R	GGTCTCACGAACATAGTATGCATGTCCGTATTTAAC	

Appendix A (*continued*)

	Gene name	Gene ID	CSP#		Sequence (5'→3')	Purpose
BraEFR2	*BraEFR2*	Bra002305	CS078	F	ggtctcAAATGAAGCCGTTTCTTTCAATTGC	Golden Gate cloning of *BraEFR2* _module 1
			CS079	R	ggtctcAAGTTCAGTGCAGTTAGTTAAACC	
			CS080	F	ggtctcAAACTAGAGTTCTTAGATGCTGG	Golden Gate cloning of *BraEFR2* _module 2
			CS081	R	ggtctcAAGGTTCAAGACTTTAACAGC	
			CS082	F	ggtctcAACCTCTTGAAGCATGGAGCAACG	Golden Gate cloning of *BraEFR2* _module 3
			CS083	R	ggtctcACGAACATTGTATGCATGTCCGCGC	
			CS237	F	GACCAAATAGCTCACTGTAATCTTAAGCCAAGCAAC	*BraEFR2* _module 3_D846N
			CS238	R	GTTGCTTGGCTTAAGATTACAGTGAGCTATTTGGTC	Mutagenesis to make dead-kinase-version
AtCERK1	*AtCERK1*	AT3G21630	CS298	F	ggtctcaGGAGGTTTCAGCTGTATGGGAAGTACC	Golden Gate cloning of *AtCERK1* promoter
			CS299	R	ggtctcaCATTTTGAAGCTTCCTTAGATTCCCC	(~ - 1000 nt)
			CS301	F	GAAACAAAAAAAACAGAGGCCCTTCCTCTGG	*AtCERK1* _modPRO_ *Bsa*I removal
			CS302	R	CCAGAGGAAGGGCCTCTGTTTTTTTTGTTTC	Mutagenesis of internal *Bsa*I in promoter module
			CS256	F	ggtctcaAATGAAGCTAAAGATTTCTCTAATCGCT	Golden Gate cloning of *AtCERK1* _module 1
			CS257	R	ggtctcaACTCCAGCACCAACACCATC	
			CS258	F	ggtctcaGAGTTATTGCTGGTATAGTTATAGGA	Golden Gate cloning of *AtCERK1* _module 2
			CS259	R	ggtctcaTGGTCTATCAAAATATTGGCAGA	
			CS260	F	ggtctcaACCAGAAATTCCGAGCAAAGG	Golden Gate cloning of *AtCERK1* _module 3
			CS291	R	ggtctcaCGAACCGGCCGGACATAAGACTG	
BraCERK1	*BraCERK1*	Bra031293	CS296	F	ggtctcaGGAGACAACAGAAGTACAATGGAAGTACC	Golden Gate cloning of *BraCERK1* promoter
			CS300	R	ggtctcaCATTTTTGATTCGTTGAGCTCTCTG	(~ - 1000 nt) (CS300: *Bsa*I removed)
			CS145	F	ggtctcaAATGGAGCTACGGATCCAAATTGC	Golden Gate cloning of *BraCERK1* _module 1
			CS122	R	ggtctcaAGGTGGGAATGTACCGTTTGG	
			CS123	F	ggtctcaACCTTTCAAGTCAAGGTAGGTTTTG	Golden Gate cloning of *BraCERK1* _module 2
			CS124	R	ggtctcaAGAGATCCCTCTACACAATAACC	
			CS125	F	ggtctcaCTCTTTTCTTGATCTATGAGTATG	Golden Gate cloning of *BraCERK1* _module 3
			CS135	R	ggtctcaCGAACCGGCCAGACATAAGGCTGAC	
			CS231	F	GAAAGCTGCAATCAAGAACATGGACATGGAGGCATC	*BraCERK1* _module 2_K349N
			CS232	R	GATGCCTCCATGTCCATGTTCTTGATTGCAGCTTTC	Mutagenesis to make dead-kinase-version

Appendix A (*continued*)

	Gene name	Gene ID	CSP#		Sequence (5'→3')	Purpose
Transgenes expression	*AtEF1α*	AT5G60390	CS038	F	CAGGCTGATTGTGCTGTTCTTA	Reference gene
			CS039	R	GTTGTATCCGACCTTCTTCAGG	
	HA tag	Hemagglutinin (98-106AA)	CS471	R	GGGATAGCCCGCATAGTCAG	Checking *BraPRR* -HA fusion expression in transgenic Arabidopsis
	BraFLS2	Bra017563	CS475	F	GGAAGCAGGAAGAGGCTGTT	
	BraEFR1	Bra006560	CS473	F	ATCGGGATGCTGTGCAAAGT	
	BraEFR2	Bra002305	CS474	F	CGGGATGCTGTGCAAAGTTC	
	BraCERK1	Bra031293	CS472	F	AAACTGGGACGTCGGAAACT	
***PRR* CAPS**	*FLS2* & homolog		CS608	F	TGATGGAGCTGATGACGAAAC	Differentiate transgenes and expression
			CS609	R	TCAGGTCTAGAGCTTGTACAG	
	EFR & homologs		CS546	F	TTTATGGCGGAATGTGAAACCT	
			CS547	R	CCCACCTGCAAAACCAGTCT	
	CERK1 & homolog		CS606	F	GTAGATGTATATGCATTTGGAGTTG	
			CS607	R	GCAACCACAATGTATCTCATACT	

Appendix B | Cloning and expression vector construction using Golden Gate assembly

(Norang: Norang Kimchi Baechu, the commercial cultivar of Chinese cabbage in Korea)

Gene	Template	Clone name	Size (nt)	Ligation	Plasmid	CSG#	Host Strain	Selection by
AtFLS2 (AT5G46330)	Col-0 gDNA	AtFLS2_mod1	1086	pUC19b/*SmaI*	pICH41021 : AtFLS2-mod1 (clone 1-5)	CSG 245	*E. coli* DH5_alpha	Amp100
		AtFLS2_mod2	1103	pUC19b/*SmaI*	pICH41021 : AtFLS2-mod2 (clone 2-2)	CSG 246	*E. coli* DH5_alpha	Amp100
		AtFLS2_mod3	1123	pUC19b/*SmaI*	pICH41021 : AtFLS2-mod3 (clone 3-1)	CSG 247	*E. coli* DH5_alpha	Amp100
		AtFLS2_mod4	303	pUC19b/*SmaI*	pICH41021 : AtFLS2-mod4 (clone 4-1)	CSG 248	*E. coli* DH5_alpha	Amp100
					pICH86988 : 35S : AtFLS2-6xHA	CSG 251	*Agrobacterium tumefaciens* AGL1	Amp100/Kan50
					pICH86988 : 35S : AtFLS2-YFP	CSG 322	*Agrobacterium tumefaciens* AGL1	Amp100/Kan50
BraFLS2 (Bra017563)	Norang gDNA	BraFLS2_mod1	1086	pUC19b/*SmaI*	pICH41021 : BraFLS2-mod1 (clone 1-1)	CSG 254	*E. coli* DH5_alpha	Amp100
		BraFLS2_mod2	1109	pUC19b/*SmaI*	pICH41021 : BraFLS2-mod2 (clone 2-1)	CSG 255	*E. coli* DH5_alpha	Amp100
		BraFLS2_mod3	1235	pUC19b/*SmaI*	pICH41021 : BraFLS2-mod3 (clone 3-7)	CSG 256	*E. coli* DH5_alpha	Amp100
		BraFLS2_mod4	300	pUC19b/*SmaI*	pICH41021 : BraFLS2-mod4 (clone 4-6)	CSG 258	*E. coli* DH5_alpha	Amp100
					pICH86988 : 35S : BraFLS2-6xHA	CSG 260	*Agrobacterium tumefaciens* AGL1	Amp100/Kan50
					pICH86988 : 35S : BraFLS2-YFP	CSG 323	*Agrobacterium tumefaciens* AGL1	Amp100/Kan50
					pICH41021 : BraFLS2-mod3_D999N (clone 3.2)	CSG 281	*E. coli* DH5_alpha	Amp100
					pICH86988 : 35S : BraFLS2_D999N-6xHA	CSG 280	*Agrobacterium tumefaciens* AGL1	Amp100/Kan50
AtEFR (AT5G20480)	Col-0 gDNA	AtEFR_mod1	1146	pUC19b/*SmaI*	pICH41021 : AtEFR_mod1	CSG 164	*E. coli* DH5_alpha	Amp100
		AtEFR_mod2	1139	pUC19b/*SmaI*	pICH41021 : AtEFR_mod2	CSG 165	*E. coli* DH5_alpha	Amp100
		AtEFR_mod3	903	pUC19b/*SmaI*	pICH41021 : AtEFR_mod3	CSG 166	*E. coli* DH5_alpha	Amp100
					pICH86988 : 35S: AtEFR-6xHA	CSG 169	*Agrobacterium tumefaciens* AGL1	Amp100/Kan50
					pICH86988 : 35S : AtEFR-YFP	CSG 324	*Agrobacterium tumefaciens* AGL1	Amp100/Kan50
BraEFR1 (Bra006560)	IDT - synthesis	BraEFR1_mod1	1113	pUC19b/*SmaI*	pICH41021 : BraEFR1-mod1 (clone 1-1)	CSG 237	*E. coli* DH5_alpha	Amp100
		BraEFR1_mod2	853	pUC19b/*SmaI*	pICH41021 : BraEFR1-mod2 (clone 2-2)	CSG 238	*E. coli* DH5_alpha	Amp100
		BraEFR1_mod3	1264	pUC19b/*SmaI*	pICH41021 : BraEFR1-mod3 (clone 3-3)	CSG 239	*E. coli* DH5_alpha	Amp100
					pICH86988 : 35S : BraEFR1-6xHA	CSG 244	*Agrobacterium tumefaciens* AGL1	Amp100/Kan50
					pICH86988 : 35S : BraEFR1-YFP	CSG 325	*Agrobacterium tumefaciens* AGL1	Amp100/Kan50

Appendix B (*continued*)

Gene	Template	Clone name	Size (nt)	Ligation	Plasmid	CSG#	Host Strain	Selection by
BraEFR2 (Bra002305)	Norang gDNA	BraEFR2_mod1	1031	pUC19b/ *Sma*I	pICH41021 : BraEFR2-mod1 (clone 1-2)	CSG 209	*E. coli* DH5_alpha	Amp100
		BraEFR2_mod2	1213	pUC19b/ *Sma*I	pICH41021 : BraEFR2-mod2 (clone 2-3)	CSG 210	*E. coli* DH5_alpha	Amp100
		BraEFR2_mod3	940	pGEM-T	pGEM-T : BraEFR2-mod3 (clone 3-1)	CSG 211	*E. coli* DH5_alpha	Amp100
					pGEM-T : BraEFR2-mod3 (clone 3-1) BsaI removed	CSG 212	*E. coli* DH5_alpha	Amp100
					pICH86988 : 35S : BraEFR2-6xHA	CSG 221	*Agrobacterium tumefaciens*	AGL1 Amp100/Kan50
					pICH86988 : 35S : BraEFR2-YFP	CSG 326	*Agrobacterium tumefaciens*	AGL1 Amp100/Kan50
					pGEM-T : BraEFR2-mod3_D846N (clone 3.2) BsaI removed	CSG 268	*E. coli* DH5_alpha	Amp100
					pICH86988 : 35S : BraEFR2_D846N-6xHA	CSG 274	*Agrobacterium tumefaciens*	AGL1 Amp100/Kan50
AtCERK1 (AT3G21630)	Col-0 gDNA	AtCERK1_mod1	983	pUC19b/ *Sma*I	pICH41021 : AtCERK1-mod1 (clone1.1)	CSG 277	*E. coli* DH5_alpha	Amp100
		AtCERK1_mod2	992	pUC19b/ *Sma*I	pICH41021 : AtCERK1-mod2 (clone2.1)	CSG 278	*E. coli* DH5_alpha	Amp100
		AtCERK1_mod3	1023	pUC19b/ *Sma*I	pICH41021 : AtCERK1-mod3 (clone3.2)	CSG 282	*E. coli* DH5_alpha	Amp100
					pICH86988 : 35S : AtCERK1-6xHA	CSG 283	*Agrobacterium tumefaciens*	AGL1 Amp100/Kan50
					pICH41021 : AtCERK1-modPRO (GGAG-AATG)	CSG 294	*E. coli* DH5_alpha	Amp100
					pICH41021 : AtCERK1-modPRO (GGAG-AATG)-BsaI removed	CSG 298	*E. coli* DH5_alpha	Amp100
					pICH86966 : pAtCERK1 : AtCERK1-6xHA	CSG 306	*Agrobacterium tumefaciens*	AGL1 Amp100/Kan50
					pICH86966 : pAtCERK1 : AtCERK1-YFP	CSG 307	*Agrobacterium tumefaciens*	AGL1 Amp100/Kan50
BraCERK1 (Bra031293)	Norang gDNA	BraCERK1_mod1	989	pUC19b/ *Sma*I	pICH41021 : BraCERK1_mod1 (clone1-1)	CSG 192	*E. coli* DH5_alpha	Amp100
		BraCERK1_mod2	919	pUC19b/ *Sma*I	pICH41021 : BraCERK1_mod2 (clone2-2)	CSG 173	*E. coli* DH5_alpha	Amp100
		BraCERK1_mod3	1101	pUC19b/ *Sma*I	pICH41021 : BraCERK1_mod3 (clone3-2)	CSG 193	*E. coli* DH5_alpha	Amp100
					pICH86988 : 35S : BraCERK1-6xHA	CSG 203	*Agrobacterium tumefaciens*	AGL1 Amp100/Kan50
					pICH41021 : BraCERK1-mod2_K349N (clone 2.2)	CSG 269	*E. coli* DH5_alpha	Amp100
					pICH86988 : 35S : BraCERK1_K349N-6xHA	CSG 275	*Agrobacterium tumefaciens*	AGL1 Amp100/Kan50
					pICH41021 : BraCERK1-modPRO (GGAG-AATG)	CSG 295	*E. coli* DH5_alpha	Amp100
					pICH86966 : pBraCERK1 : BraCERK1-6xHA	CSG 296	*Agrobacterium tumefaciens*	AGL1 Amp100/Kan50
					pICH86966 : pBraCERK1 : BraCERK1_K349N-6xHA	CSG 338	*Agrobacterium tumefaciens*	AGL1 Amp100/Kan50
					pICH86966 : pBraCERK1 : BraCERK1-YFP	CSG 297	*Agrobacterium tumefaciens*	AGL1 Amp100/Kan50

Appendix C | Generation of *Arabidopsis* transgenic *PRR* expressing lines

Line	Insert gene construct	Background plant	T1	T2	T2 (R:S)	T3 (homozygous)
F1	*35S : AtFLS2-6xHA*	*fec*	14	F1-1 → F1-12	F1-1 (21:1)	
					F1-2 (5.24:1)	
F2	*35S : BraFLS2-6xHA*	*fec*	2	F2-1	F2-1 (2.26:1)	
F3	*35S : BraFLS2_D999N-6xHA*	*fec*	12	F3-1 → F3-11	F3-1 (4.53:1)	
					F3-2 (4.52:1)	
					F3-3 (2.69:1)	
					F3-4 (11.5:1)	
F4	*35S : AtFLS2-6xHA*	*fls2*	12	F4-1 → F4-12	F4-1 (2.93:1)	F4-1-1
					F4-2 (2.60:1)	
					F4-3 (R<<S)	
					F4-4 (0.86:1)	
					F4-5 (13.4:1)	
					F4-6 (2.66:1)	
					F4-7 (2.40:1)	
F5	*35S : BraFLS2-6xHA*	*fls2*	11	F5-1 → F5-9	F5-1 (2.22:1)	
					F5-2 (2.06:1)	
					F5-3 (R<<S)	
					F5-4 (100% R)	
					F5-6 (3.31:1)	
					F5-7 (8.86:1)	
F6	*35S : BraFLS2_D999N-6xHA*	*fls2*	16	F6-1 → F6-16	F6-1 (R<<S)	
					F6-2 (3.57:1)	
					F6-3 (2.20:1)	
					F6-4 (R<<S)	
					F6-5 (3.69:1)	
					F6-6 (4.04:1)	

Appendix C (*continued*)

Line	Insert gene construct	Background plant	T1	T2	T2 (R:S)	T3 (homozygous)
E1	*35S : AtEFR-6xHA*	*fec*	6	E1-1 → E1-6	E1-1 (3.51:1) E1-2 (11.38:1) E1-3 (2.90:1) E1-4 (2.6:1) E1-5 (21:1)	E1-1-2
E2	*35S : BraEFR1-6xHA*	*fec*	10	E2-1 → E2-10	E2-1 (2.03:1) E2-3 (60.5:1) E2-4 (3.97:1) E2-5 (3.32:1) E2-6 (3.64:1) E2-7 (3.71:1)	E2-4-2 E2-5-5
E4	*35S : BraEFR2-6xHA*	*fec*	30	E4-1 → E4-30	E4-1 (3.06:1) E4-2 (2.95:1) E4-3 (3.29:1) E4-4 (2.21:1) E4-5 (2.63:1)	E4-1-5 E4-4-1 E4-4-2
E5	*35S : BraEFR2_D846N-6xHA*	*fec*	21	E5-1 → E5-13	E5-1 (17.7:1) E5-2 (R<<S) E5-3 (2.43:1) E5-4 (9.5:1)	E5-1-1

Appendix C (*continued*)

Line	Insert gene construct	Background plant	T1	T2	T2 (R:S)	T3 (homozygous)
C1	*35S : AtCERK1-6xHA*	*fec*	1	C1-1	C1-1 (2.52:1)	
C2	*35S : BraCERK1-6xHA*	*fec*	4	C2-1 → C2-4	C2-1 (100% S) C2-2 (2.17:1) C2-3 (2.74:1) C2-4 (2.67:1)	
C3	*35S : BraCERK1_K349N-6xHA*	*fec*	7	C3-1 → C3-7	C3-2 (4.58:1) C3-3 (2.4:1) C3-4 (2.22:1) C3-5 (2.93:1)	
C4	*pAtCERK1 : AtCERK1-6xHA*	*fec*	18	C4-1 → C4-18	C4-1 (3.11:1) C4-2 (14.4:1) C4-3 (2.33:1) C4-4 (5.44:1)	
C5	*pBraCERK1 : BraCERK1-6xHA*	*fec*	13	C5-1 → C5-12	C5-1 (1.91:1) C5-2 (4.93:1) C5-3 (2.55:1)	
C6	*pBraCERK1 : BraCERK1_K349N-6xHA*	*fec*	9	C6-1 → C6-6	C6-1 (37.4:1) C6-2 (25:1)	

- R:S indicated the ratios of resistant to susceptible individuals on kanamycin medium

- *fec* indicated *fls2 efr cerk1* mutant

초록

배추 (*Brassica rapa* spp. *pekinensis*)는 중요한 원예 작물의 하나로 국내에서 인기가 많다. 배추의 생산에 있어 가장 큰 피해는 박테리아와 곰팡이로부터 발생하며, 이 때문에 면역체계에 대한 관련 연구가 활발히 일어나고 있다. 식물은 병원체로부터 자신을 보호하기 위해 선천적인 면역계에 의존한다. 세포 표면에 있는 패턴 인식 수용체 (PRR; Pattern-Recognition Receptor)는 flagellin, elongation factor Tu 혹은 곰팡이 세포벽 성분 chitin 같은 병원체 관련 분자 패턴 (PAMP; Pathogen-Associated Molecular Pattern)을 인지하고 패턴 유발 면역 (PTI; Pattern Triggered Immunity)이라고 불리는 일련의 방어 반응을 유도한다. PTI 는 병원체의 성장을 효율적으로 억제시키고 내구성이 있는 광범위한 스펙트럼의 질병에 대한 저항성을 제공한다. 모델 식물 애기장대에서 PRR 과 PTI 에 대해 연구가 집중적으로 되었지만, 배추에서는 포괄적인 연구가 많이 부족하다.

이에 본 연구는 배추의 PTI 분자적 기초를 탐구하기 위해 대표적인 방어반응을 평가함으로 PAMP 대응성을 조사하였다. 우선 신뢰성 있는 마커 유전자 *BraNHL10* 을 발견 및 확인하였다. *BraNHL10* 은 여러 PAMP 에 의해 그 발현이 현저하고 신속하게 유도되었다. ROS 생산은 배추에서 flg22, elf18 및 chitin 처리시 신속하게 유도됨을 확인할 수 있었다.

비교분석 결과 애기장대의 *FLS2*, *EFR*, *CERK1* 의 첨가 호몰로그가 *B. rapa* 게놈에 존재하며, BraPRR 과 AtPRR 의 단백질 배열이 높은 유사성을 보이는 것으로 나타났다. 그 다음으로 *BraFLS2*, *BraEFR1*, *BraEFR2* 및 *BraCERK1* 를 골든 게이트 클로닝 전략으로 복제한 후 *Nicotiana benthamiana* 에서 BraFLS2, BraEFR1, BraEFR2 및 BraCERK1 의 일시적인 발현을 통해 모든 BraPRRs 이 세포막에 정착함을 확인할 수 있었으며,

BraFLS2 발현에 따라 flg22 처리시 endocytosis 가, *BraEFR2* 발현에 따라 elf18 처리시 ROS burst 가, *BraCERK1* 발현에 따라 chitin 처리와 무관한 세포예정사가 유발되었다. *BraEFR1* 의 발현은 *N. benthamiana* 에서 ROS burst 을 유도하지 않았으므로 BraEFR1은 기능하지 않는 것으로 추정되었다.

이어서 *BraFLS2, BraEFR1, BraEFR2* 및 *BraCERK1* 이 애기장대 단일 돌연변이 *fls2* 혹은 트리플 돌연변이 *fls2 efr cerk1* 에서 진행한 기능보완시험을 통해 기능을 재확인하였다. *BraFLS2, BraEFR2* 및 *BraCERK1* 의 발현은 flg22, elf18 및 chitin 에 대한 인식과 관련된 면역 반응을 각각 보완하였다. *BraFLS2* 와 *BraEFR2* 의 발현으로 형질전환 식물에서 각각 flg22 및 elf18 으로 유도된 묘목 성장 억제를 보였다. *BraFLS2, BraEFR2* 및 *BraCERK1* 의 발현은 형질전환체에서 flg22, elf18 및 chitin 처리시 또 각각 ROS 생산을 유도하였다. 그리고 BraPRR 의 kinase 활성이 부여한 기능을 연구하기 위해 *BraPRR* 의 dead kinase 버전을 구축해서 면역 반응을 평가하였다.

이 모든 결과로부터 BraFLS2, BraEFR2 및 BraCERK1 이 배추에서 PRR 역할을 담당하고 그들의 기능은 kinase 의 활성에 부분적 의지하고 있을 것으로 추정되었다.